

# Renewable Energy

## Hierarchically porous PTSA with Si species for efficient and sustainable conversion of non food castor oil to biodiesel

--Manuscript Draft--

<b>Manuscript Number:</b>	
<b>Article Type:</b>	Research Paper
<b>Keywords:</b>	Castor oil, fatty acid methyl ester, heterogeneous catalyst, transesterification, p-toluene sulfonic acid, calorific value.
<b>Corresponding Author:</b>	Bharat Z Dholakiya, Ph.D SVNIT, Surat Surat, INDIA
<b>First Author:</b>	Bharat Z Dholakiya, Ph.D
<b>Order of Authors:</b>	Bharat Z Dholakiya, Ph.D Dr. Mehulkumar L. Savaliya, Ph.D Er. Ravi S. Tank, B.E Chemical
<b>Abstract:</b>	Catalysis is the vertebra of most of commercial processes, which utilizes chemical reactions to transform reagents into value added chemicals. Biodiesel synthesis from animal fats and edible vegetable oils via transesterification over homogeneous catalysts is recently taken into account of untenable by the emerging biofuel industries, particularly by virtue of food vs. fuel counteraction, economic and environmental challenges blended with the feedstocks as well as catalytic systems, respectively. Therefore, present efforts concern with the preparation of a novel PTSA-Si catalyst and its relevance for biodiesel synthesis from non-food castor oil. It has been manifested from the experimental outcomes, the most relevant reaction parameters are, 5 % PTSA-Si (w/w) , 65 °C reaction temperature, 1:11 O:M molar ratio and 10 h reaction time for 98.56 % biodiesel yield. The PTSA-Si was appropriately analyzed using FT-IR, SEM, XRD, BET, TGA-DTA and TPD-NH <sub>3</sub> analysis. Since, castor oil and castor biodiesel were analyzed using FT-IR, <sup>1</sup> H & <sup>13</sup> C-NMR analysis. Besides, biodiesel physico-chemical properties were predicted and associated with ASTM fuel standards.
<b>Suggested Reviewers:</b>	Dr. Ramesh L. Gardas, Ph.D Professor, Indian Institute of Technology Madras gardas@iitm.ac.in He has enough expertise in the biofuel.  Dr. Pragnesh N Dave, Ph.D Professor, Sardar Patel University pragneshdave@gmail.com He bears good experience in the catalysis.

# Hierarchically porous PTSA with Si species for efficient and sustainable conversion of non food castor oil to biodiesel

Mehulkumar L. Savaliya<sup>a,b</sup>, Ravi S. Tank<sup>a</sup> and Bharatkumar Z. Dholakiya<sup>b\*</sup>

---

<sup>a</sup>*Faculty of Science, Department of Industrial Chemistry, Atmiya University, Yogidham Gurukul, Kalawad road, Rajkot-360005, Gujarat, India.*

<sup>b</sup>*Department of Chemistry, Sardar Vallabhbhai National Institute of Technology (SVNIT), Ichchhanath, Surat-395007, Gujarat, India.*

**\*Corresponding Author.** Tel No:- +91 9428949595, Fax- 0261 227334,

E-mail address: [bharat281173@gmail.com](mailto:bharat281173@gmail.com), [mehulkumar.savaliya@atmiyauni.ac.in](mailto:mehulkumar.savaliya@atmiyauni.ac.in),

[ravi.tank@atmiyauni.ac.in](mailto:ravi.tank@atmiyauni.ac.in)

---

## ***Abstract***

Catalysis is the vertebra of most of commercial processes, which utilizes chemical reactions to transform reagents into value added chemicals. Biodiesel synthesis from animal fats and edible vegetable oils via transesterification over homogeneous catalysts is recently taken into account of untenable by the emerging biofuel industries, particularly by virtue of food vs. fuel counteraction, economic and environmental challenges blended with the feedstocks as well as catalytic systems, respectively. Therefore, present efforts concern with the preparation of a novel PTSA-Si catalyst and its relevance for biodiesel synthesis from non-food castor oil. It has been manifested from the experimental outcomes, the most relevant reaction parameters are, 5 % PTSA-Si (w/w), 65 °C reaction temperature, 1:11 O:M molar ratio and 10 h reaction time for

98.56 % biodiesel yield. The PTSA-Si was appropriately analyzed using FT-IR, SEM, XRD, BET, TGA-DTA and TPD-NH<sub>3</sub> analysis. Since, castor oil and castor biodiesel were analyzed using FT-IR, <sup>1</sup>H & <sup>13</sup>C-NMR analysis. Besides, biodiesel physico-chemical properties were predicted and associated with ASTM fuel standards.

**Keywords-** Castor oil, fatty acid methyl ester, heterogeneous catalyst, transesterification, *p*-toluene sulfonic acid, calorific value.



सरदार वल्लभभाई राष्ट्रीय प्रौद्योगिकी संस्थान, सूरत  
Sardar Vallabhbhai National Institute of Technology

Date: 19/06/2022

To,  
The Editor in Chief,  
**Renewable energy**

**Sub- Submission research article**

Respected sir

Herewith, I am sending a research article entitled **“Hierarchically porous PTSA with Si species for efficient and sustainable conversion of non food castor oil to biodiesel”** for the possible publication in Renewable energy. It consists of 22 pages of manuscript. It also consist 12 figures and 06 tables along with one supplementary file.

The manuscript has not been previously published, is not currently submitted for review to any other journal and will not be submitted elsewhere before a decision is made by this journal.

All authors have declared that they have no any conflict/competing of interest.

We would be grateful if you could review it and consider it for publication.

Yours sincerely,

**Corresponding author,**

Dr. B. Z. Dholakiya, PhD

Associate Professor,

Department of Chemistry,

Sardar Vallabhbhai National Institute of Technology, Surat-395007, (Gujarat), India. (M)

+91 9428949595,

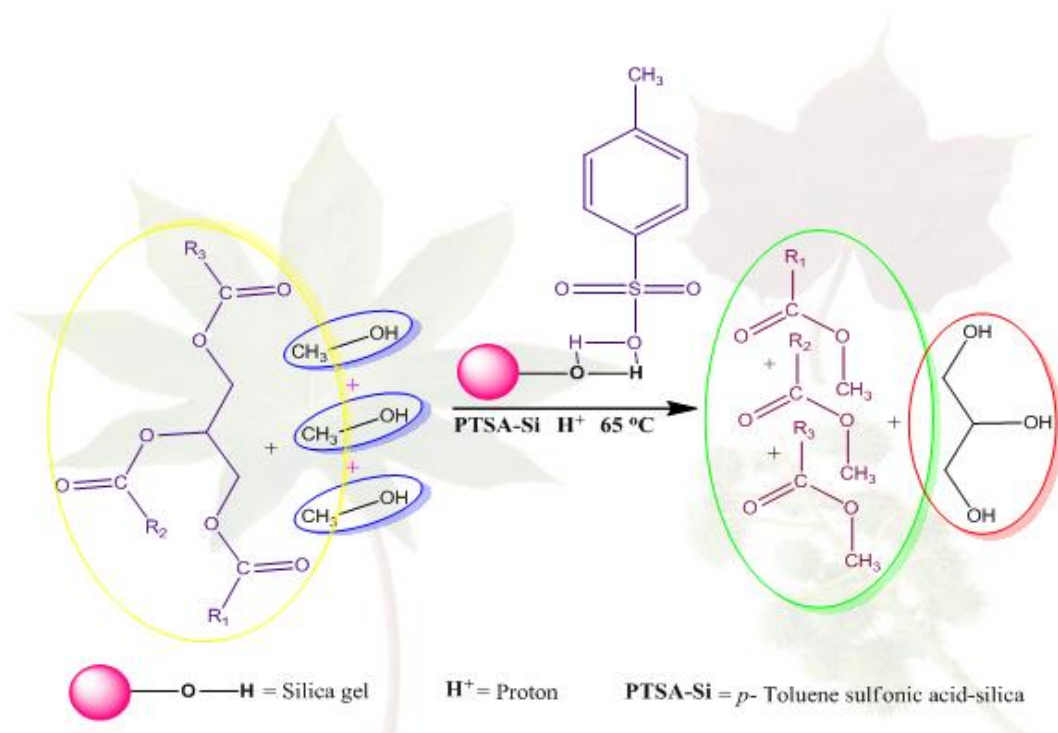
E-mail: [bharat281173@gmail.com](mailto:bharat281173@gmail.com)

## Ethical Statement

Present work deals with the synthesis of a novel PTSA-Si catalyst and its application for biodiesel preparation using non-food castor oil (CO). It has been manifested from the experimental results, the optimum reaction parameters are, 1:11 oil to methanol molar ratio, 5 % PTSA-Si (*w/w*), 65 °C reaction temperature and 10 h reaction time for 98.56 % yield of biodiesel. The PTSA-Si was appropriately analyzed using FT-IR, SEM, XRD, BET, TGA-DTA and TPD-NH<sub>3</sub> analysis. However, castor oil and castor biodiesel (CB) were analyzed using FT-IR, <sup>1</sup>H & <sup>13</sup>C-NMR analysis. Besides, fuel properties of biodiesel were measured and correlated with ASTM fuel standards.

The manuscript has not been previously published, is not currently submitted for review to any other journal and will not be submitted elsewhere before a decision is made by this journal.

## Graphical abstract



***Highlights for review***

1. Preparation of *p*-toluene sulfonic acid-silica catalyst via sulfonation of toluene.
2. Synthesis of economical biodiesel via transesterification of non edible castor oil using PTSA-Si catalyst.
3. Comparison of catalytic performance of PTSA-Si with reported solid acid catalysts.
4. Estimation of fuel properties of castor biodiesel and comparison with ASTM fuel standards.
5. Estimation of thermal stability and moisture absorption capacity of PTSA-Si.

# Hierarchically porous PTSA with Si species for efficient and sustainable conversion of non food castor oil to biodiesel

Mehulkumar L. Savaliya<sup>a,b</sup>, Ravi S. Tank<sup>a</sup> and Bhartkumar Z. Dholakiya<sup>b\*</sup>

---

<sup>a</sup>Faculty of Science, Department of Industrial Chemistry, Atmiya University, Yogidham Gurukul, Kalawad road, Rajkot-360005, Gujarat, India.

<sup>b</sup>Department of Chemistry, Sardar Vallabhbhai National Institute of Technology (SVNIT), Ichchhanath, Surat-395007, Gujarat, India.

\*Corresponding Author. Tel No:- +91 9428949595, Fax- 0261 227334,

E-mail address: [bharat281173@gmail.com](mailto:bharat281173@gmail.com), [mehulkumar.savaliya@atmiyauni.ac.in](mailto:mehulkumar.savaliya@atmiyauni.ac.in),

[ravi.tank@atmiyauni.ac.in](mailto:ravi.tank@atmiyauni.ac.in)

---

## Abstract

Catalysis is the vertebra of most of commercial processes, which utilizes chemical reactions to transform reagents into value added chemicals. Biodiesel synthesis from animal fats and edible vegetable oils via transesterification over homogeneous catalysts is recently taken into account of untenable by the emerging biofuel industries, particularly by virtue of food vs. fuel counteraction, economic and environmental challenges blended with the feedstocks as well as catalytic systems, respectively. Therefore, present efforts concern with the preparation of a novel PTSA-Si catalyst and its relevance for biodiesel synthesis from non-food castor oil. It has been manifested from the experimental outcomes, the most relevant reaction parameters are, 5 % PTSA-Si (w/w), 65 °C reaction temperature, 1:11 O:M molar ratio and 10 h reaction time for 98.56 % biodiesel yield. The PTSA-Si was appropriately analyzed using FT-IR, SEM, XRD, BET, TGA-DTA and TPD-NH<sub>3</sub> analysis. Since, castor oil and castor biodiesel were analyzed using FT-IR, <sup>1</sup>H & <sup>13</sup>C-NMR analysis.



24 Besides, biodiesel physico-chemical properties were predicted and associated with ASTM  
25 fuel standards.

26 **Keywords-** Castor oil, fatty acid methyl ester, heterogeneous catalyst, transesterification, *p*-  
27 toluene sulfonic acid, calorific value.

## 28 ***1.0. Introduction***

29

30 The wind, solar and biomass energy are potential substitute in the direction of petroleum  
31 based fuels and are excellent commercial sources of renewable energy [1]. The insistence of  
32 biofuels as a green fuel is accelerated advancement in the last decennium with a view to  
33 reduce our obsession on petroleum based fuels as a leading source of transportation fuel as  
34 per the Kyoto protocol on emission control of greenhouse gases [2]. Biofuels are compounds  
35 originated from biomass that could directly be a substitute for, or be used as mixture with  
36 conventional transportation fuels [3]. The biodiesel is a class of biofuel that could be  
37 prepared from variety of feedstocks, assorted into three main groups (i) vegetable oils, (ii)  
38 animal fats and (iii) waste frying oils [4]. A fourth group of developing attention are the algal  
39 oils offering great oil productiveness. However, the utilization of algal oil as an alternative is  
40 still very finite due to high attributed expenses [5]. Presently, cooking oils are being used in  
41 more than 95% of the global biodiesel preparation [6]. The major sense behind utilization of  
42 cooking oil for biodiesel preparation is that they are easily accessible from massive  
43 agricultural formulation enterprises. Nonetheless, this is not a favourable direction due to the  
44 significant percussions on food chain inviting to the so known as food vs. fuel conflict [7]. To  
45 date, considerable non food oils have also been examined as raw materials for biodiesel  
46 preparation along with seed oils of jatropha curcas, calo-phyllum inophyllum, tobacco,  
47 rubber, mahua, karanja, castor and schleichera oleosa [8]. Among all the oil crops, the castor  
48 oil has the considerable oil yield capacity. It offers the higher yield of seeds and oil

49 compositions in its seeds. The major composition of ricinoleic acid is responsible for the  
50 higher viscosity and density of castor oil. It has a potential to get dissolved in alcohol, which  
51 favours the transesterification reaction. The main sense behind selection of castor oil as  
52 feedstocks for biodiesel preparation in present study is its higher production in India, lower  
53 economical cost and relevant fuel properties [9]. The physicochemical properties of castor oil  
54 are listed in Table 1.

55 **<Table 1.>**

56 An interest of biodiesel as a green option to conventional fuel comprise its engine  
57 affinity and higher engine wear, high transportability, easily availability, eco-friendliness,  
58 better combustion performance, better energy generation, low sulphur and aromatic  
59 compositions, leading cetane index and greater biodegradability [12]. The combustion of  
60 biodiesel offers more than 90% decrease in the total unspent hydrocarbons and a 75-90%  
61 weakens cyclic aromatic hydrocarbons emission related to the utilization of petroleum based  
62 fuels. Biodiesel also demonstrates a noteworthy shrinkage in particulates matters as well as  
63 CO with respect to fossil fuel [13]. The biodiesel is being prepared by using homogeneous  
64 alkali and acidic catalysts like, KOH, NaOH, H<sub>2</sub>SO<sub>4</sub>, HCl and HNO<sub>3</sub> [14]. However, the  
65 biodiesel preparation using heterogeneous catalysts contributes a potential substitutive way  
66 for their economical production [15]. Solid acids offer several intrinsic advantages over liquid  
67 counterparts such as, easy separation, simple post treatment, less waste emission and higher  
68 thermal stability [16-17]. Many solid acids have been developed to compensate the  
69 conventional liquid acids catalysts. However, most of the solid acid catalysts are less stable,  
70 less active and more expensive than the liquid acid catalysts [18]. Solid acid catalysts offer  
71 economic and process benefits, especially for low cost feedstocks with high FFA content,  
72 enabling single step esterification and transesterification of bio oils [19]. A wide range of  
73 solid acids including heteropolyacids heteropolyacids [20-22], sulfonated metal oxides [23-

74 24], carbons [25], and zeolites [26] have been employed for biodiesel preparation,  
75 nevertheless, novel materials with tailored solvothermal stability and recyclability are still  
76 sought. Mesoporous solid acid catalysts are attractive in heterogeneous catalysis with a view  
77 to their tunable pore architectures, high surface areas, associated improved mass-transport  
78 and potential to generate highly dispersed and active sites [27]. There are several reports  
79 available for the single step biodiesel preparation from waste oils using solid acids, including  
80 carbon based solid acid [28], active clay [29], Zr-SBA-15 [30] and sulfated tin oxide [31].  
81 The waste oils contain FFAs and triglycerides; both of them form biodiesel. Several benefits  
82 of biodiesel in association with petroleum based diesel are that it is environment friendly and  
83 safer to use, as it is being prepared from sustainable resources and contains little amounts of  
84 sulfur. Even though, the cold flow assets, NO<sub>x</sub> discharge and higher production expenses are  
85 major countenance that have to be defeated [32].

86

87         With the above considerations, a novel heterogeneous acid catalyst of silica fused *p*-  
88 toluene sulfonic acid was freshly prepared by chemical and physical modification of toluene  
89 and silica gel respectively. The synthesized PTSA-Si was examined for single step biodiesel  
90 production via transesterification of non food castor oil. It has been concluded from the  
91 transesterification results of non food castor oil, the excellent experimental parameters for the  
92 maximum biodiesel yield (98.56 %) are, 5 % PTSA-Si (*w/w*), 65 °C reaction temperature,  
93 1:11 O:M molar ratio and 10 h reaction span. The synthesized PTSA-Si has been assessed for  
94 repeatability study and commenced to be four time successfully reusable without loss of their  
95 catalytic performance. The castor oil biodiesel has also been examined for their physico-  
96 chemical properties estimation. It has been observed from the study that all physico-chemical  
97 properties are found to be within limits prescribed by ASTM standards.

98

99

100

## 101 **2.0. Materials and method**

### 102 **2.1. Materials**

103 The methanol ( $\geq 99.0\%$ , EMPLURA), silica gel (96.1%, 60-120 mesh), toluene  
104 ( $\geq 99.0\%$ , EMPLURA), sodium sulphate (99.0%, FINAR), sulfuric acid (99.9%, RANKEM),  
105 methylene dichloride (99.8%, FINAR) and *n*-hexane (99.9%, FINAR) were furnished by  
106 Aashka Scientific Co., Surat, Gujarat. The castor oil was purchased from local oil trader  
107 (Malhar trading), Surat, Gujarat, India. All reagent utilized in the present study were of  
108 analytical grade and employed without additional purification.

### 109 **2.2. Instrumental techniques**

110 The FT-IR spectrum PTSA-Si was executed on a FT-IR spectrometer (Shimadzu).  
111 However, the FT-IR analysis of castor oil and castor biodiesel were carried out on another  
112 FT-IR spectrometer (Perkin-Elmer). The  $^1\text{H-NMR}$  and  $^{13}\text{C-NMR}$  analyses were done on a  
113 FT-NMR spectrometer (Bruker 400 MHz NMR). The castor biodiesel (%) yield was  
114 calculated on GC analysis (YL 6500GC, SUPELCO C<sub>8</sub>- C<sub>24</sub> FAME mixture). The wide angle  
115 X-ray diffraction pattern was recorded on XRD (Rigaku). The specific surface area of PTSA-  
116 Si was predicted on a porosimeter (2020, ASAP). The thermal strength of PTSA-Si was  
117 identified by TGA (Perkin Elmer). The superficial morphologies of PTSA-Si were  
118 recognized by SEM (S3400N, Hitachi). The total bronsted acid sites in the PTSA-Si were  
119 predicted by TPD-NH<sub>3</sub> analysis (Chemisorb 2750).

### 120 **2.3. Experimental**

#### 121 **2.3.1. Synthesis of PTSA-Si**

122 The PTSA-Si has been prepared by little modification of the reported method [33]. A  
123 100 mL of toluene and 20 mL of concentrated sulfuric acid were transferred in a 250 mL  
124 glass reactor (FBF, adapted with a dean stark assembly). The flask was heated with reflux at  
125 160 °C for 6 h. The water droplets began to produce at the same time as a starting of the  
126 sulfonation reaction. The quantity of water collected in the dean stark collector was measured  
127 at regular interval of times. On the completion of 5 h of sulfonation, a 12.1 mL of water was  
128 measured and the sulfonation was extended as far as no further water was produced. On the  
129 completion of sulfonation, the heating was interrupted and reaction mass was acquiesced to  
130 cool at ambient temperature. The crystallization of *p*-toluene sulfonic acid (PTSA) has been  
131 carried out through addition of 30 mL of distilled water. The PTSA has been isolated from  
132 the reaction mass and washed with again 10 mL of water. The PTSA has been purified by  
133 dissolving in small amount of hot water containing activated charcoal. Finally, the PTSA has  
134 been recovered from the aqueous slurry and cooled with ice. A treatment of gaseous HCl to  
135 this supper cooled solution leads to the precipitation of white crystals of PTSA (40.18 g).  
136 Then after, an equimolar quantity of silica gel was mixed to these white crystals and  
137 mechanically stirred at room temperature for 1 h to support PTSA-Si via induction of  
138 intermutual hydrogen bonding [34]. Ultimately, a 53.25 g freshly dried light gray fine powder  
139 of PTSA-Si was achieved. The reaction strategy for production of PTSA-Si is embossed in  
140 Fig 1.

141 <Fig. 1>

### 142 **2.3.2. Catalytic performance test**

143 The transesterification of castor oil was functioned out in 250 mL flat bottom flask,  
144 which was adapted with reflux condenser, magnetic stirrer and heating plate system. The  
145 required amounts of castor oil, % PTSA-Si (*w/w*) and methanol were calculated  
146 stoichiometrically. The desired amount of castor oil was added to flat bottom flask followed

147 by charging of PSTA-Si-methanol mixture. The reflux temperature (65 °C) was maintained  
148 and reaction assembly were left uninterrupted for required time period. After the desired  
149 length of reaction time, the reaction mixture was carefully shifted to the partition funnel for  
150 the partition of the product and by product. The separating funnel was again left  
151 uninterrupted till the complete separation of biodiesel and glycerol layers as depicted in Fig  
152 S1. The glycerol collected at the bottom was separated first. The hot distilled water and  
153 anhydrous sodium sulphate were used for the refining of biodiesel layer. Consciously to  
154 investigate the significance of reaction parameters on the (%) yield of transesterification  
155 products, the reactions were carried out by changing catalyst concentration (1, 2, 3, 4, 5 and  
156 6% w/w), O:M molar ratio (1:9, 1:10, 1:11 and 1:12) and reaction time (6, 7, 8, 9 and 10 h) at  
157 reflux temperature (65 °C). All experiments have been executed in triplicates with a view to  
158 find deviations in the biodiesel yield (%) after each successful experiment. The scheme for  
159 the transesterification of castor oil has been demonstrated in Fig. 2.

160

161

<Fig. 2>

### 162 **2.3.3. Biodiesel (%) yield estimation**

163 The castor biodiesel (%) yields and their fatty acid methyl esters distribution were  
164 measured through GC investigation. The C<sub>8</sub>- C<sub>24</sub> composition biodiesel mixture (SUPELCO)  
165 was involved as a measure for qualitative and quantitative persistence of biodiesel  
166 composition on GC (specification: (30 m × 0.320 mm × 0.25 µm, FID, column: Agilent DB-  
167 Wax-123-7032)). The peak areas have been accounted for the projection of fatty acid methyl  
168 esters composition of each castor biodiesel sample after fatty acid methyl esters of the castor  
169 biodiesel samples were identified. The conversion and (%) biodiesel yield were calculated by  
170 following formula (i) and (ii) [35].

171 
$$C = \frac{\sum A - A_{IS}}{A_{IS}} \times \frac{C_{IS} \times V_{IS}}{m} \times 100 \dots \dots \dots (i)$$

172 Where,  $C$  stand for the fatty acid methyl ester content,  $\sum A$  represent the total peaks  
 173 area,  $A_{IS}$  refers to the methyl heptadecanoate (internal standard) peak area,  $C_{IS}$  and  $V_{IS}$  stands  
 174 for the concentration (mg/mL) and volume of internal standard (mL) respectively. The  $m$   
 175 stand for the quantity of the castor biodiesel (mg).

176

177 
$$\text{Castor biodiesel yield (\%)} = \frac{M_{\text{Biodiesel}} \times C}{M_{\text{Oil}}} \times 100 \dots \dots \dots (ii)$$

178 Where  $M_{\text{Biodiesel}}$  represent the quantity of refined fatty acid methyl esters obtained,  
 179  $M_{\text{Oil}}$  stand for the quantity of castor oil selected and  $C$  stand for the fatty acid methyl ester  
 180 content estimated as mentioned through equation (i). It has been found from the gas  
 181 chromatogram of castor biodiesel, the prepared biodiesel is offers several methylated fatty  
 182 acids like methyl ricinoleate, methyl oleate, methyl linoleate and methyl stearate. The GC-  
 183 FID chromatogram of castor biodiesel is mentined in Fig. S2.

184 **2.3.4. Mechanism of transesterification of castor oil over PTSA-Si**

185 It has been already reported the transesterification of triglycerides (oil) are being  
 186 catalyzed by either acidic or alkaline catalysts. It involves three successive reversible  
 187 reactions. It has been observed that in the transesterification reaction chain, the triglycerides  
 188 is transformed stepwise to diacylglycerol, monoacylglycerol and followed by glycerine,  
 189 which is associated with the production of one mole of biodiesel at each stage [20]. The  
 190 mechanism of castor oil transesterification also follows the same sequence. These steps  
 191 composed of (i) Protonation ( $H^+$ ) of one of the carbonyl group of castor oil through the  
 192 PTSA-Si (ii) Nucleophilic incursion of the methanol pointing to the carbonyl group that yield  
 193 a tetrahedral transitional product and (iii) Proton displacement ( $H^+$ ) and disconnection of the

194 tetrahedral intermediate yields biodiesel and diacylglycerol. The displaced proton repeatedly  
195 consumed through the leading PTSA-Si with a view to reproduce it for the next repetitive  
196 use. This consolidated continuity will repeat by two times till thorough synthesis of mixture  
197 of biodiesel and glycerol. The mechanism scheme for the transesterification of castor oil is  
198 given in Fig. 3.

199 <Fig. 3>

### 200 **3.0. Results and discussion**

201 Generally, the transesterification of oil demands a suitable catalyst with a view to obtain  
202 desired production rates. The constitution of the catalyst is remains essential since it regulate  
203 the configurations restrictions that the raw material must contain. Besides, the reaction  
204 parameters and post isolation steps are pre-planned by the attributes of the catalyst employed  
205 [36]. Generally, majority of oils are being transformed into biodiesel using alkali catalyzed  
206 transesterification method. But there are several uncommon cases wherein direct  
207 transesterification cannot be carried out. Such cases appear in raw vegetable oils like olive,  
208 jatropha, castor and cotton seed oil, etc. Such raw vegetable oils possess high free fatty acids  
209 (FFAs) contents in their oil compositions, as it forms soap on base catalyzed  
210 transesterification [10]. Therefore, it is a demand of time to develop an efficient  
211 heterogeneous acid catalyst to overcome such problems. Because, the heterogeneous acid  
212 catalysts can concurrently conducts transesterification of TGs and esterification of FFAs to  
213 biodiesel. Hence, it is not required to isolate free fatty acids from the triglycerides [36]. With  
214 the above considerations, in the present study, the biodiesel synthesis has been carried out by  
215 transesterification of non food castor oil over PTSA-Si as a solid acid catalyst. In order to  
216 optimize the process parameters, the biodiesel reactions were examined by varying catalyst  
217 concentration (1, 2, 3, 4, 5 and 6% w/w), O:M molar ratio (1:9, 1:10, 1:11 and 1:12) and  
218 reaction time (6, 7, 8, 9 and 10 h) at reflux temperature (65 °C). All the experiments were



219 functioned at viscerous pressure till an attainment of the maximum conversions. The results  
220 of castor biodiesel yields (%) with distinctive reaction parameters have been tabularized in  
221 Table 2.

222 < Table 2.>

223 **3.1. Influence of oil to methanol molar ratio**

224 In pursuance to look into the cause of oil to methanol (O:M) molar ratio on biodiesel  
225 (%) yields, all reactions were executed out at diverse O:M molar ratio (1:9, 1:10, 1:11 and  
226 1:12). In connection with Table 2, it has been confirmed that, the biodiesel yield (%) is  
227 precisely influence by diversifying methanol to oil (M:O) molar ratio. The biodiesel (%) yield  
228 is gradually increased with the increasing M:O molar ratio. With 1:9, 1:10, 1:11 and 1:12  
229 O:M molar ratio, the maximum biodiesel (%) yields were found to be 80.23 %, 88.12 %, 98.56 %  
230 and 94.23 % respectively. The optimal biodiesel (%) yield (98.56 %) was found with  
231 1:11 O:M molar ratio. The backward reaction (alcoholysis of glycerol and biodiesel) directly  
232 enhances upon keeping O:M molar ratio down from 1:11. Accordingly, the reversible nature  
233 of the transesterification is the responsible factor for the decrement in (%) yield of biodiesel  
234 at O:M molar ratio below 1:11. It has also been perceived that the reduction in the biodiesel  
235 (%) yield above 1:11 O:M molar ratio and this may in conjunction to the polar apparent of  
236 PTSA-Si and methyl alcohol. Wherefore, it constantly raises the polarity of the  
237 transesterification, on increasing of M:O molar ratio. In advance of, the reaction mechanism  
238 of transesterification evidently acclaimed that, first oil must react with catalyst. Though, as  
239 the quantity of alcohol increases, the reaction mass is also starts to increase its polarity.  
240 Therefore, contrary to oil aspect, the PTSA-Si constantly displaced to the alcohol aspect.  
241 Wherefore, the connections of PTSA-Si in the direction of methanol phase become absolutely  
242 energetic than connections of PTSA-Si in the direction of oil phase. Consequently, the  
243 shrinkage in the biodiesel (%) yield was noticed above 1:11 O:M molar ratio. The bar graph

244 indicating an effect of O:M molar ratio approaching biodiesel (%) yield is manifested in Fig.  
245 4.

246 **< Fig.4>**

### 247 **3.2. Influence of reaction time (h)**

248 In pursuance to look into the effect of reaction span (h) in direction of biodiesel (%)  
249 yield, all experiments were studied employing diversified span of reaction times (6, 7, 8, 9  
250 and 10 h). In connection with Table 2, it has been perceived that the 1:11 O:M molar ratio  
251 demonstrates optimum yield of biodiesel (98.56 %). Thus, 1:11 O:M molar ratio was  
252 preferred as an optimal ratio to examine biodiesel synthesis employing diversified span of  
253 reaction times. From the observations, it can be evidenced that, with 6 h, 7 h, 8 h, 9 h and 10  
254 h reaction times, the optimal biodiesel (%) yields observed were 68.54 %, 80.29 %, 88.65 %, 91.32 %  
255 and 98.56 % respectively. alongside 10 h reaction time, it indicates almost complete  
256 conversion of castor oil into biodiesel, thus, the reaction time (h) was not studied beyond 10 h  
257 span. The bar graph indicating an effect of reaction time (h) approaching biodiesel (%) yield  
258 has been manifested in Fig. 5.

259 **< Fig. 5>**

### 260 **3.3. Influence of PTSA-Si quantity (% w/w)**

261 In pursuance to look into the cause of PTSA-Si quantity (% w/w) on biodiesel (%)  
262 yields, all experiments were executed by shifting PTSA-Si concentration (1, 2, 3, 4, 5 and 6%  
263 w/w). In connection with Table 2, it was realized that, the biodiesel (%) yield increases on  
264 increasing the catalyst quantity (% w/w). In the case of 1 %, 2 %, 3 %, 4 %, 5 % and 6 %  
265 catalyst quantity (w/w), the biodiesel (%) yield were found to be 22.34 %, 38.35 %, 54.23 %, 82.56,  
266 98.56 % and 98.24 % respectively at optimum O:M molar ratio. The PTSA-Si quantity  
267 above 5 % (w/w) doesn't symbolize any noticeable improvement in the biodiesel (%) yield

268 rather the (%) yield of biodiesel is slight decreased with 6 % catalyst due to increment of the  
269 polarity of the reaction on increment of the % catalyst (*w/w*). Accordingly, it was observed  
270 from the reaction outcomes, as catalyst quantity (% *w/w*) increases, the biodiesel (%) yield  
271 also increases. The bar graph indicating an effect of PTSA-Si quantity (% *w/w*) approaching  
272 biodiesel (%) yield is manifested Fig. 6.

273 < Fig. 6.>

#### 274 **3.4. FT-IR analysis of PTSA-Si**

275 The FTIR spectroscopy is a precise technique being used particularly for identifying  
276 organic chemicals in a whole range of applications. An absorption pattern of synthesized  
277 PTSA-Si catalyst is accustomed by the existence of characteristic bands at 3439.19  $\text{cm}^{-1}$   
278  $^1$ (stretching, intermolecular H- bonding, O-H), 3036.06  $\text{cm}^{-1}$  (stretching, C-H), 2918.40  $\text{cm}^{-1}$   
279 (stretching,  $\text{CH}_3$ ), 1629.90  $\text{cm}^{-1}$  (bending, C=C), 1206.33  $\text{cm}^{-1}$  (stretching, C-S), 1143.83  $\text{cm}^{-1}$   
280  $^1$  (stretching, O=S=O (by virtue of  $-\text{SO}_3\text{H}$  group)), 1066.67  $\text{cm}^{-1}$  (stretching, S=O), 1016.52  
281  $\text{cm}^{-1}$  (stretching, O-Si-O), 815.92  $\text{cm}^{-1}$  (*p*-substituted benzene ring) and 692.47  $\text{cm}^{-1}$  (bending,  
282 C-H) subsequently. The FT-IR graph of PTSA-Si is mentioned in Fig. 7.

283 <Fig 7.>

#### 284 **3.5. Morphological study of PTSA-Si catalyst**

285 An external morphology and structural orientation of PTSA-Si has been studied by  
286 scanning electron microscopic analysis. It has been observed from the SEM micrographs of  
287 PTSA-Si catalyst, the PTSA particles are found with aggregates of irregular size and shapes  
288 after sulfonation with sulphuric acid. Whereas, the silica gel particles are found with finer  
289 needles of pentagonal shape. It has been well reported that silica particles are found to have  
290 smoother surface. However, on treatment with *p*- toluene sulfonic acid, they are found with  
291 rough surface. The average particle size of PTSA-Si has been found in the range of 1.07-1.66

292  $\mu\text{m}$ . Muthu *et al.* (2014) have synthesized sulfated zirconia catalyst via solvent free method  
293 and evaluated for the biodiesel synthesis using neem oil. From the SEM micrograph of  
294 sulfated zirconia, they realized that the particle size of sulphated zirconia is in the range of  
295 20-30 $\mu\text{m}$  and is in an agglomerated form on calcination at 600 °C [37]. The SEM  
296 micrographs of PTSA-Si are picturized in Fig. 8.

297 **<Fig 8.>**

### 298 **3.6. The crystalline structure of the PTSA-Si**

299 The texture characteristics of PTSA-Si were analyzed by X- ray diffraction analysis.  
300 The X-Ray diffractogram displayed characteristics diffraction pattern showing crystalline  
301 nature of PTSA-Si. The diffractogram displayed particular diffraction impression confirming  
302 crystalline texture of PTSA-Si. The particular peaks recognized at  $2\theta = 9.22$  (deg.) (face-  
303 centered cubic),  $2\theta = 13.04$  (deg.) (body-centered cubic),  $2\theta = 15.14$  (deg.) (face-centered  
304 cubic/ diamond cubic),  $2\theta = 16.84$  (deg.) (body-centered cubic/ simple cubic),  $2\theta = 18.10$   
305 (deg.) (face-centered cubic/ simple cubic),  $2\theta = 22.12$  (deg.) (simple cubic),  $2\theta = 24.08$  (deg.)  
306 (body-centered cubic),  $2\theta = 24.62$  (deg.) (body-centered cubic),  $2\theta = 25.60$  (deg.) (body-  
307 centered cubic/ simple cubic),  $2\theta = 27.16$  (deg.) (body-centered cubic),  $2\theta = 28.12$  (deg.)  
308 (face-centered cubic) and  $2\theta = 76.16$  (deg.) (face-centered cubic) are associated with the  
309 existence of silica gel crystals (JCPDS-29-1129). Although, knife-edged peaks observed at  $2\theta$   
310 = 31.74 (deg.),  $2\theta = 34.02$  (deg.),  $2\theta = 38.42$  (deg.),  $2\theta = 42.92$  (deg.),  $2\theta = 43.72$  (deg.),  $2\theta =$   
311 45.80 (deg.) and  $2\theta = 52.68$  (deg.) are peculiarity of *p*-toluene sulfonic acid (JCPDS-39-  
312 1699). The wide angle X-Ray diffractogram of PTSA-Si has been demonstrated in Fig. 9.

313 **<Fig. 9.>**

### 314 **3.7. Determination of thermal stability**

315 The thermal strength of the PTSA-Si was assured by TGA examination. The weight  
316 loss of PTSA-Si was measured as behaviour of raise in temperature or heating rate. The  
317 TGA-DTA curve of PTSA-Si displays a natural three stage disintegration diagram. The three  
318 steps in disintegration diagram can be predicted by loss of moisture, decomposition of  
319 sulfonic acid group (-SO<sub>3</sub>H) and total degradation and decomposition of PTSA. The first  
320 weight loss (10.68 %) is observed in temperature domain of 30 to 150 °C is due to  
321 disintegration of absorbed moisture on catalyst surface. The second weight loss (45.03 %) is  
322 observed in temperature domain of 150 to 400 °C is accredited with the disintegration of  
323 sulfonic acid groups (-SO<sub>3</sub>H) of the toluene. The second derivative of DTA also confirms the  
324 disintegration of sulfonic acid groups from the toluene. However, the third weight loss (5.49  
325 %) is observed in temperature domain of 400 to 910 °C is an account for the decomposition  
326 of toluene. In the present study all transesterification reactions have been carried out at reflux  
327 temperature (65 °C). However, in the TGA curve of PTSA-Si, it was recognized that the first  
328 weight loss (10.68 %) is observed in temperature scale of 30 to 150 °C is due to disintegration  
329 of absorbed moisture on PTSA-Si surface. Hence, the PTSA-Si offers a better thermal  
330 stability at reflux temperature. Ferreira e Santos *et al.* (2014) have prepared a novel ZrO<sub>2</sub>-  
331 SiO<sub>2</sub> mixed oxides and evaluated for the thermal stability study. From the TGA thermogram  
332 of ZrO<sub>2</sub>-SiO<sub>2</sub> mixed oxides, they found that the almost constant decrease of mass in the scale  
333 of 100 to 200 °C, which is due to the decomposition of water, impurities, alkoxides, and  
334 unspent solvents. Although, beyond 700 °C temperature, the weight loss is accredited to the  
335 dehydroxilation of the catalyst framework [38]. The TGA thermogram of PTSA-Si is  
336 depicted in Fig. 10.

337 <Fig. 10 >

338

339

340 **3.8. Determination of surface area of PTSA-Si**

341 The specific surface area of PTSA-Si was executed by Brunauer-Emmet-Teller (BET)  
342 surface area analysis and the results are tabularized in Table 3.

343 < Table 3.>

344 From the BET isotherm of PTSA-Si, it has been observed that the catalyst offers a  
345 specific surface area of 9.61 m<sup>2</sup>/g, pore volume of 0.99 cm<sup>3</sup>/g and pore size of 2.50 nm. The  
346 lower pore volume and pore size itself express that the existence of sulfonic acid (-SO<sub>3</sub>H)  
347 groups on the porous surface of PTSA-Si catalyst. The hysteresis of PTSA-Si has been found  
348 typically of type-IV, which indicates the presence of mesoporous structure of PTSA-Si. This  
349 conclusion is also identical with reported literature [39]. Ferreira e Santos *al.* have prepared a  
350 novel ZrO<sub>2</sub>-SiO<sub>2</sub> mixed oxides and evaluated for the specific surface area determination.  
351 They observed that the catalyst offers a specific surface area of 1742 m<sup>2</sup>/g and BET  
352 isotherm found of type- IV indicating the presence of mesoporous structure of ZrO<sub>2</sub>-SiO<sub>2</sub>  
353 mixed oxides [38]. The BET isotherm of PTSA-Si has been demonstrated in Fig. 11.

354 <Fig. 11 >

355 **3.9. Determination of acidity of PTSA-Si**

356 The total active sites (H<sup>+</sup>) in PTSA-Si were measured using TPD-NH<sub>3</sub> analysis and  
357 results are tabularized in Table 4.

358 < Table 4.>

359 In connection to the TPD-NH<sub>3</sub> spectrum of PTSA-Si, it was found that the catalyst  
360 offers a bronsted acidity of 1.49 mmol/g at 194.8 °C, which confirms the presence of  
361 acid/super acid sites on the PTSA-Si surface. Ferreira e Santos *et al.* have prepared a novel  
362 ZrO<sub>2</sub>-SiO<sub>2</sub> mixed oxides and evaluated for the total acidity determination by TPD-NH<sub>3</sub>

363 analysis. From the TPD-NH<sub>3</sub> spectrum of ZrO<sub>2</sub>-SiO<sub>2</sub> mixed oxides, they observed that the  
364 catalyst offers an acidity of 476 mmol/g, which affirmed the existence of acid/super acid  
365 sites on the sulfonated materials [38]. The TPD-NH<sub>3</sub> spectrum of PTSA-Si is demonstrated  
366 in in Fig. S3.

### 367 **3.10. FT-IR analysis of CO**

368 The FT-IR spectrum of castor oil (CO) is accustomed with the presence of  
369 characteristics bands at 2926.01 cm<sup>-1</sup> (CH<sub>3</sub> stretching), 2852.72 cm<sup>-1</sup> (CH<sub>2</sub> stretching),  
370 2029.11 cm<sup>-1</sup> (C=C stretching), 1743.65 cm<sup>-1</sup> (C=O stretching), 1462.04 cm<sup>-1</sup> (CH bending),  
371 1163.08 cm<sup>-1</sup> and 1095.57 (C-O stretching) and 725.23 cm<sup>-1</sup> (CH rocking) respectively. The  
372 FT-IR spectrum of CO is illustrated in Fig. S4 (a).

373

### 374 **3.11. FT-IR analysis of CB**

375 The FT-IR spectrum of castor biodiesel (CB) is accustomed with the presence of an  
376 essential bands at 2926.01 cm<sup>-1</sup> (CH<sub>3</sub> stretching), 2854.65 cm<sup>-1</sup> (CH<sub>2</sub> stretching), 2046.47 cm<sup>-1</sup>  
377 (C=C stretching), 1737.86 cm<sup>-1</sup> (C=O stretching), 1460.11 and 1436.97 cm<sup>-1</sup> (CH bending),  
378 1195.87, 1172.72 cm<sup>-1</sup> and 1012.63 cm<sup>-1</sup> (C-O stretching) and 725.23 cm<sup>-1</sup> (CH rocking)  
379 respectively. The FT-IR spectrum of CB is illustrated in Fig. S4 (b).

380

### 381 **3.12. <sup>1</sup>H-NMR analysis CO**

382 The proton nuclear magnetic resonance (<sup>1</sup>H-NMR) is a spectroscopic technique  
383 generally used for structural determination of organic molecules. The structure of castor oil  
384 was accustomed by an essential peaks at 5.33-5.40 ppm (unsaturated olefinic -CH=CH-  
385 protons), 4.24-4.39 ppm (CH-CH<sub>2</sub> protons), 4.11 ppm (O-CH<sub>2</sub> protons), 3.35-3.39 ppm (-OH  
386 protons), 2.50 ppm (α-CH<sub>2</sub> protons), 2.23-2.28 ppm (β-CH<sub>2</sub> protons) and 2.02-2.09 ppm (CH<sub>3</sub>  
387 protons) respectively. The <sup>1</sup>H-NMR spectrum of CO is illustrated in Fig. S5 (a).

388

### 389 **3.13. <sup>1</sup>H-NMR analysis CB**

390 The structure of castor biodiesel was accustomed by the presence of an essential  
391 peaks at 7.28 ppm (CDCl<sub>3</sub> solvent), 5.28-5.50 ppm (unsaturated olefinic -CH=CH- protons),  
392 4.81-4.84 ppm (CH-CH<sub>2</sub> protons), 3.54-3.60 ppm (CH<sub>3</sub>O-methoxy protons), 2.22-2.26 ppm  
393 (α-CH<sub>2</sub> protons) and 2.14-2.21 ppm (β-CH<sub>2</sub> protons) respectively. The <sup>1</sup>H-NMR spectrum of  
394 CB is illustrated in Fig. S5 (b).

395

### 396 **3.14. <sup>13</sup>C-NMR analysis of CO**

397 The structure of castor oil was also accustomed by the presence of an essential peaks  
398 at 171.98-172.31 ppm (C=O carbons), 126.58-130.26 ppm (olefinic carbons), 69.72 ppm  
399 (CH-O carbons), 68.69 ppm (CH<sub>2</sub>-O carbons), 61.73 ppm (CH<sub>3</sub> carbon), 36.45-40.08 ppm  
400 (DMSO solvent) and 28.39-36.45 ppm (aliphatic carbons) respectively. The <sup>13</sup>C-NMR  
401 spectrum of CO is illustrated in Fig. S6 (a).

402

### 403 **3.15. <sup>13</sup>C-NMR analysis of CB**

404 The structure of castor biodiesel is also accustomed by the presence of an essential  
405 peaks at 173.50-176.38 ppm (C=O carbons), 124.27-132.90 ppm (olefinic carbons), 76.82-  
406 77.45 ppm (CDCl<sub>3</sub>- solvent), 63.28-73.62 ppm (CH-O carbons), 51.37 ppm (O-CH<sub>3</sub> carbon)  
407 and 27.31-36.78 ppm (aliphatic carbons) respectively. The <sup>13</sup>C-NMR spectrum of synthesized  
408 CB is illustrated in Fig. S6 (b).

409

410

### 411 **3.16. Comparison of catalytic exertion of PTSA-Si**



412 The resemblance of catalytic activity of any catalyst is of significant important in  
413 order to ensure the activity of synthesized catalysts with existing literature [36]. Further, it  
414 also helps to design an economical viable production process. Table 5 represents the  
415 resemblance of catalytic activity of PTSA-Si with outcomes of existing literature for the  
416 equivalent class of heterogeneous bronsted acid catalysts examined for biodiesel production  
417 through castor oil transesterification.

418 <Table 5>

419 From Table 5 it was ascertained that PTSA-Si offers noteworthy catalytic execution  
420 for the transesterification of castor oil as a means of biodiesel synthesis. In current  
421 investigation, the fundamental reaction parameters found for the maximum biodiesel yield  
422 (%) are; 65 °C reaction temperature, 1:11 O:M molar ratio, 5 % (w/w) PTSA-Si and 10 h  
423 reaction span, for 98.56 % biodiesel conversion. It was also been established from Table 5,  
424 the outcomes of the current investigation are conveniently corresponding to the outcomes of  
425 existing literature for the identical class of heterogeneous bronsted catalysts, where  
426 analogously rigorous reaction conditions were demanded [42, 45-48].

427 **3.17. Moisture absorption sensitivity of PTSA-Si**

428 The synthesized PTSA-Si was also evaluated for their moisture absorption sensitivity.  
429 Therefore, herein, the prescribed quantity of PTSA-Si was transferred in a glass bottle which  
430 kept in stabile wetness at room temperature for certain days with a view to permit the  
431 moisture absorption on the PTSA-Si catalyst. The PTSA-Si catalyst was weighed at regular  
432 slot of times. The moisture absorption rate (W%) of the PTSA-Si catalyst was determined  
433 through following formula (iii).

434 
$$W\% = \left[ \frac{56 \Delta m}{18m_0} \right] \times [100] \dots \dots \dots (iii)$$

435           Where,  $\Delta m$  belongs to the increased weight and  $m_0$  belongs to the initial weight of the  
436 PTSA-Si sample. The impact of moisture exposure time (h) on the moisture absorption rate  
437 of PTSA-Si is illustrated in Fig. S7.

438           From Fig. S7, it was examined that, the moisture absorption profile is continuously  
439 increasing alongside increasing in the moisture revelation span (h) up to 90 h. However,  
440 beyond 90 h of moisture exposure time (h), the PTSA-Si doesn't display any noteworthy  
441 intensification in its weight. It is almost saturated by the atmospheric moisture. The *p*-  
442 toluene sulfonic acid (PTSA) surface present a one hydroxyl (-OH) groups in conjunction to  
443 one sulfonic (-SO<sub>3</sub>H) acid group in their framework. Therefore, due to polar composition of  
444 PTSA-Si, it holds a tendency to freely consume the moisture against steady humidity  
445 atmosphere.

### 446 ***3.18. Influence of repetitive runs of PTSA-Si on castor biodiesel (%) yield***

447           The production expense of biodiesel itself decides their accessible and large scale  
448 commercialization [36]. The catalyst reusability is a considerable feature for the measurement  
449 of an economical viability of the production process. Therefore, with an intention to cut down  
450 an economical expense of biodiesel production, the PTSA-Si was evaluated for their possible  
451 recyclability in the castor oil transesterification. Accordingly, in present work, after each  
452 successful cycle, the PTSA-Si was detached out from the reaction batch by means of vacuum  
453 separation and mediated with few quantity of methylene dichloride with a view to expel  
454 impurities like, unused castor oil, glycerol and unused alcohol. Before the repetitive use, the  
455 purified PTSA-Si was putted up in an air dryer at 100 °C for 24 h with a view to remove  
456 volatile solvent and regeneration of active centres (H<sup>+</sup>) on the toluene surface. It was  
457 observed through execution of castor oil transesterification, the PTSA-Si could have a  
458 significant potential to recycle four times left out characteristic desertion of catalytic  
459 performance. This reusability might be due to the stability of PTSA-Si and the strong

460 attachment of sulfonic acid group (-SO<sub>3</sub>H) with toluene. Nonetheless, the minor reduction in  
461 the (%) yield of castor biodiesel has been noticed during the repetitive cycles of PTSA-Si. An  
462 extraction of active site (H<sup>+</sup>) or physicochemical change of PTSA-Si framework at 65 °C  
463 temperature could responsible for the deactivation of PTSA-Si. The toluene sustains its  
464 structure over the castor oil transesterification without any severe change. The virgin PTSA-  
465 Si could displays optimum conversion of castor oil to biodiesel equal to 98.56 %. While, it's  
466 first, second, third and fourth repetitive run could displays optimum transformations of oil to  
467 biodiesel up to 94.25 %, 90.26 %, 86.28 % and 81.20 % subsequently. Liu *et al.* (2008) have  
468 synthesized sulfonated ordered mesoporous carbon (OMC-SO<sub>3</sub>H) and examined for biodiesel  
469 synthesis through esterification of oleic acid. From the reusability study of the OMC-SO<sub>3</sub>H  
470 catalyst, they concluded that the OMC-SO<sub>3</sub>H catalyst can be reusable for four successful  
471 times without noticeable loss of catalytic exertion. They also concluded that the reusability is  
472 due to the thermal stability of OMC-SO<sub>3</sub>H and the strong coupling of sulfonic acid group  
473 with carbon [49]. An impact of PTSA-Si runs on the biodiesel (%) yield is exemplified in  
474 Fig.12.

475 **<Fig 12.>**

### 476 ***3.19. Assessment of fuel properties of castor biodiesel***

477 The castor oil plant grows in a hot and humid environment; it has a growing season of 4-5  
478 months. The castor oil is a colourless to very pale yellow viscous liquid with moderate or no  
479 odour or taste. Castor oil offers a very lower pour and cloud points which make castor  
480 biodiesel a good alternative in winter season [50]. The physico-chemical properties of  
481 biodiesel can diversify considerably from one raw material to another owing to its somewhat  
482 high molecular mass than conventional diesel. The considerable fuel standard systems like  
483 ASTM, AOCS, IS, JIS, BS and EU are fruitful for the correlation of the physico-chemical  
484 properties of biodiesel produced from diversified oils. The physico-chemical properties are

485 useful for any fuel to determine their engine performance, emission, storage and  
486 transportations conditions. The fuel properties of castor biodiesel with contrast to ASTM  
487 standards have been tabularized in Table 6.

488

489

**<Table 6.>**

490 The cetane number was measured on cetane analyser (AFIDA 2805). The density of  
491 castor biodiesel was measured by hydrometer mechanism. The acid and iodine values have  
492 been measured by titration methods. The specific gravity of biodiesel has been calculated  
493 using specific gravity bottles. Flash and fire points were predicted by closed cup tester  
494 (ADITYA-SUNBIM). The refractive index has been measure by refractometer (Anton parr,  
495 abbemat 300). The cloud and pour points have been determined on cloud and pour point  
496 analyzer (ALANready, CPP 5Gs). The calorific value of castor biodiesel has been determined  
497 through oxygen bomb calorimeter (Parr 6400 calorimeter). The kinematic viscosity and  
498 viscosity were measured on viscometer (Aditya 01). From Table 6, it was recognized that all  
499 physico-chemical properties of castor biodiesel are according to the test restrictions, which  
500 are established by ASTM standards.

501 ***3.20. Industrial aspect of the process***

502 An economical viability is very necessary with a view to explore preparation of  
503 biodiesel at commercial spectrum [36,51]. When small-scale manufacturers embark on  
504 survey of the finances of biodiesel production, they frequently discover it complex to acquire  
505 oil at a lower cost for cost-effective production. The oil is the potential contributor to the cost  
506 (more than 80 %) of biodiesel manufacturing [36,51]. Fresh oil obtained from an oilseed  
507 manufacturer tends to be the chief quality, most consistent and easily available. However, it  
508 also is expected to be a very costly resource of vegetable oil. The biodiesel reaction absorbs

509 11% methanol (% w/w) in the transesterification process. Nonetheless, most manufacturers  
510 utilize between 18-22% methanol to certify a more complete conversion and make use of all  
511 quantity of oil during reaction. Small-scale biodiesel production economics can vary  
512 considerably depending on specific manufacturer's selection of oil source, machinery,  
513 merchandise and the expense of manpower. However, several fundamental controversies  
514 affect all small-scale manufacturers. Thus, Present work will deals with the usage of non-  
515 edible castor oil as an oil source for biodiesel preparation, because of non-edibility, the castor  
516 oil is cheap and readily available in the oil market. In addition, reusability of PTSA-Si will be  
517 taken in to the account, as heterogeneous class of catalyst. The preparation cost for PTSA-Si  
518 would not involve large cost with a view to only single step sulfonation is carried out for its  
519 preparation. Therefore, this process would offers an economical biodiesel manufacturing  
520 using milder reaction parameters.

#### 521 ***4.0. Conclusion***

522

523 In current investigation, a promising four time reusable PTSA-Si is freshly prepared  
524 and investigated for transesterification of castor oil regarding biodiesel production. It has  
525 been manifested against the reaction outcomes; the better relevant reaction parameters for  
526 biodiesel synthesis as a means of transesterification of castor oil are; 5 % PTSA-Si (w/w), 65  
527 °C reaction temperature, 1:11 O:M molar ratio and 10 h reaction time for 98.56 % biodiesel  
528 yield. In view of synchronously conduction of an esterification and transesterification by  
529 PTSA-Si catalyst, thus, it is not significant to segregate FFAs from castor oil and therefore, it  
530 yields economical biodiesel with appreciated conversion.

#### 531 ***Acknowledgement***

532 Authors are very much thankful to the S.V. National Institute of Technology, Surat  
533 and CSIR, New Delhi, India (Sanction Order Letter No. 02(0170)/13/EMR-II) for financial

534 compensation. We are extremely thankful to the Mechanical Engineering Department,  
535 SVNIT, Surat, Department of Chemistry, IIT Madras and Prof. Anamik Shah, Center of  
536 Excellence in Drug Discovery, Saurashtra University, Rajkot, Gujarat, India for analytical  
537 instrumentation facility.

538

### 539 *Conflict/competing of interest*

540 The authors declare that they have no known competing financial interests or personal  
541 relationships that could have appeared to influence the work reported in this paper.

542

### 543 *References*

544

- 545 1. N. Izadyar, Resource assessment of the renewable energy potential for a remote area:  
546 a review, *Renew Sust Energy Rev* 62 (2016) 908-923.
- 547 2. J.A. Melero, J.Iglesias, G.Morales, Heterogeneous acid catalysts for biodiesel  
548 production: current status and future challenges, *Green Chemistry* 11 (2009) 1285-  
549 1308.
- 550 3. P.M. Schenk, Second generation biofuels: high-efficiency microalgae for biodiesel  
551 production, *Bioenergy Res* 1 (2008) 20-43.
- 552 4. I.B. Bankovic-Ilic, O.S. Stamenkovic, V.B. Veljkovic, Biodiesel production from  
553 non-edible plant oils, *Renew Sust Energy Rev* 16 (2012) 3621-3647.
- 554 5. C.Y. Chen, K.L. Yeh, R. Aisyah, D.J. Lee, J.S. Chang, Cultivation, photobioreactor  
555 design and harvesting of microalgae for biodiesel production: a critical review,  
556 *Bioresour Technol* 102 (2011) 71-81.
- 557 6. M.M. Gui, K.T. Lee, S. Bhatia, Feasibility of edible oil vs. non-edible oil vs. Waste  
558 edible oil as biodiesel feedstock, *Energy* 33 (2008) 1646-1653.

- 559 7. M. Balat, Potential alternatives to edible oils for biodiesel production-a review of  
560 current work, *Energy Convers Manag* 52 (2011) 1479-1492.
- 561 8. H. Ong, Production and comparative fuel properties of biodiesel from non- edible  
562 oils: *jatropha curcas*, *sterculia foetida* and *ceiba pentandra*, *Energy Convers Manage*  
563 73 (2013) 245-55.
- 564 9. D. Rajagopal, Rethinking current strategies for biofuel production in India, in:  
565 International Conference on Linkages in Water and Energy in Developing Countries  
566 Organized by IWMI and FAO, ICRISAT, Hyderabad, India, (2007), January 29-30.
- 567 10. R. Sattanathan, Production of biodiesel from castor oil with its performance and  
568 emission test, *International Journal of Science and Research* 4 (2015) 273-279.
- 569 11. P. Sreenivas, R.M. Venkata, K. Chandra Sekhar, Development of biodiesel from  
570 castor oil, *International journal of energy science* 3 (2011) 192-197.
- 571 12. A. Demirbas, Economic and environmental impacts of biofuels: a review, *Appl*  
572 *Energy* 86 (2009) 108-17.
- 573 13. A. Demirbas, Importance of biodiesel as transportation fuel, *Energy Policy* 35 (2007)  
574 4661-4670.
- 575 14. D.Y.C. Leung, Y. Guo, Transesterification of neat and used frying oil: optimization  
576 for biodiesel production, *Fuel Process Technol*, 87 (2006) 883-890.
- 577 15. Di Serio, M. Cozzolino, M. Giordano, M. Tesser, R. Patrono, P. Santacesaria, E.,  
578 From homogeneous to heterogeneous catalysts in biodiesel production, *Ind, Eng.*  
579 *Chem. Res.* 46 (2007) 6379-6384.
- 580 16. A. Kamal , G. Chouhan, Investigations towards the chemoselective thioacetalization  
581 of carbonyl compounds by using ionic liquid [bmim]Br as a recyclable catalytic  
582 medium, *Adv Synth Catal* 346 (2004) 579-582.

- 583 17. J.S. Yadav, B.V.S. Reddy, G. Kondaji, Eco-friendly and highly chemoselective 1,3-  
584 oxathio- and 1,3-dithioacetalization of aldehydes using ionic liquids, *Chem Lett* 32  
585 (2003) 672-673.
- 586 18. S.H. Xuan, S.F. Lee, J.T.F. Lau, X.M. Zhu, Y.X. Wang, F. Wang, Photocytotoxicity  
587 and magnetic relaxivity responses of dual-porous  $\gamma\text{-Fe}_2\text{O}_3$  @meso-SiO<sub>2</sub>  
588 microspheres, *ACS Appl Mater Interfaces* 4 (2012) 2033-2040.
- 589 19. I.A.L. Bassan, D.R. Nascimento, R.A.S. Gil, M.I.P. da Silva, C.R. Moreira, W.A.  
590 Gonzalez, A.C. Faro Jr., T. Onfroy, E.R. Lachter, Esterification of fatty acids with  
591 alcohols over niobium phosphate, *Fuel Process Technol* 106 (2013) 619-624.
- 592 20. E. Lotero, Y. Liu, D.E. Lopes, K. Suwannakarn, D.A. Bruce, J.G. Goodwin, Synthesis  
593 of biodiesel via acid catalysis, *Ind. Eng Chem Res* 44 (2005) 5353-5363.
- 594 21. K. Narasimharao, D.R. Brown, A.F. Lee, A.D. Newman, P.F. Siril, S.J. Tavener, K.  
595 Wilson, Structure-activity relations in Cs-doped heteropolyacid catalysts for biodiesel  
596 production, *J Catal* 248 (2007) 226-234.
- 597 22. L. Pesaresi, D.R. Brown, A.F. Lee, J.M. Montero, H. Williams, K. Wilson, Cs-doped  
598 H<sub>4</sub>SiW<sub>12</sub>O<sub>40</sub> catalysts for biodiesel applications, *Appl Catal A: Gen* 360 (2009) 50-58.
- 599 23. J. Dhainaut, J.P. Dacquin, A.F. Lee, K. Wilson, Hierarchical macroporous-  
600 mesoporous SBA-15 sulfonic acid catalysts for biodiesel synthesis, *Green Chem* 12  
601 (2010) 296-303.
- 602 24. C. Pirez, A.F. Lee, J.C. Manayil, C.M.A. Parlett, K. Wilson, Hydrothermal saline  
603 promoted grafting: a route to sulfonic acid SBA-15 silica with ultra-high acid site  
604 loading for biodiesel synthesis, *Green Chem.* 16 (2014) 4506-4509.
- 605 25. X. Mo, E. Lotero, C. Lu, Y. Liu, J.G. Goodwin, A novel sulfonated carbon composite  
606 solid acid catalyst for biodiesel synthesis, *Catal Lett* 123 (2008) 1-6.



- 607 26. R. Purova, K. Narasimharao, N.S.I. Ahmeda, S. Al-Thabaiti, A. Al-Shehri, M.  
608 Mokhtar, W. Schwieger, Pillared HMCM-36 zeolite catalyst for biodiesel production  
609 by esterification of palmitic acid, *J Mol Catal A: Chem* 406 (2015) 159-167.
- 610 27. A. Corma, From microporous to mesoporous molecular sieve materials and their use  
611 in catalysis, *Chem Rev* 97 (1997) 2373-2420.
- 612 28. Q. Shu, Z. Nawaz, J. Gao, Y. Liao, Q. Zhang, D. Wang, Synthesis of biodiesel from a  
613 model waste oil feedstock using a carbon-based solid acid catalyst: reaction and  
614 separation, *Bioresour Technol* 101 (2010) 5374-5384.
- 615 29. M.A. Olutoye, B.H. Hameed, A highly active clay-based catalyst for the synthesis of  
616 fatty acid methyl ester from waste cooking palm oil, *Appl Catal A: Gen* 450 (2013)  
617 57-62.
- 618 30. J.A. Melero, L.F. Bautista, J. Iglesias, G. Morales, R. Sánchez-Vázquez, Zr-SBA-15  
619 acid catalyst: optimization of the synthesis and reaction conditions for biodiesel  
620 production from low-grade oils and fats, *Catal Today* 195 (2012) 44-53.
- 621 31. M.K. Lam, K.T. Lee, A.R. Mohamed, Sulfated tin oxide as solid superacid catalyst  
622 for transesterification of waste cooking oil: an optimization study, *Appl Catal B:  
623 Environ* 93 (2009) 134-139.
- 624 32. M.R. Monteiro, A.R.P. Ambrozini, L.M. Liao, A.G. Ferreira, Determination of  
625 biodiesel blend levels in different diesel samples by <sup>1</sup>H NMR, *Fuel* 88 (2009) 691-  
626 696.
- 627 33. Y.K. Yurev, Preparation of *p*-toluene sulfonic acid, *Practical work in organic  
628 chemistry 1* (1964) 138-139.
- 629 34. M. Vafaejadeh, A. Fattahi, Calculating the acidity of silica supported alkyl sulfonic  
630 acids considering the matrix effect: A DFT study. *Phosphorous sulfur and silicon* 189  
631 (2014) 849-857.

- 632 35. P. Garcia Moreno, M. Khanum, A. Guadix, E.M. Guadix, Optimization of biodiesel  
633 production from waste fish oil, *Renewable Energy* 68 (2014) 618-624.
- 634 36. B. Z. Dholakiya, Super phosphoric acid catalyzed biodiesel production from low cost  
635 feedstock, *Archives of Applied Science Research*, 4 (2012) 551-561.
- 636 37. H. Muthu, V. Sathya Selvabala, T. K. Varathachary, D. Kirupha Selvaraj, J.  
637 Nandagopal and S. Subramanian, synthesis of biodiesel from neem oil using sulfated  
638 zirconia via transesterification, *Brazilian Journal of Chemical Engineering*, 27 (2010)  
639 601-608.
- 640 38. M.A. Ferreira e Santos, I. Pinheiro Lobo, R. Serpa da Cruz, Synthesis and  
641 Characterization of Novel ZrO<sub>2</sub>-SiO<sub>2</sub> mixed oxides, *Materials Research* 17 (2014)  
642 700-707.
- 643 39. S. Brunauer, P.H. Emmett, E. Teller, Adsorption of gases in multimolecular layers. *J*  
644 *Am Chem Soc* 60 (1938) 309-315.
- 645 40. G. Baskar, S. Soumiya, Production of biodiesel from castor oil using iron (II) doped  
646 zinc oxide Nano catalyst, *Renewable Energy* 98 (2016) 101-107.
- 647 41. N.A. Negm, G.H. Sayed, F.Z. Yehia, O. Habib, E.A. Mohamed, Biodiesel production  
648 from one-step heterogeneous catalyzed process of Castor oil and Jatropha oil using  
649 novel sulphonated phenyl silane montmorillonite catalyst, *J Mol Liq* 234 (2017) 157-  
650 163.
- 651 42. N.A. Negm, G.H. Sayed, O.Habib, F.Z. Yehia, E.A. Mohamed, Heterogeneous  
652 catalytic transformation of vegetable oils into biodiesel in one-step reaction using  
653 super acidic sulfonated modified mica catalyst, *J Mol Liq* 237 (2017) 38-45.
- 654 43. A. Drelinkiewicz, Z. Kalemba-Jaje, E. Lalik, A. Zieba, D. Mucha, E.N. Konyushenko,  
655 J. Stejskal, Transesterification of triacetin and Castor oil with methanol catalyzed by  
656 supported polyaniline-sulfate. A role of polymer morphology, *Appl Catal A* 455  
657 (2013) 92-106.

- 658 44. T.M. Serra, D.R. de Mendonça, J.P.V. da Silva, M.R. Meneghetti, S.M. Plentz  
659 Meneghetti, Comparison of soybean oil and castor oil methanolysis in the presence of  
660 tin (IV) complexes, *Fuel* 90 (2011) 2203-2206.
- 661 45. A. Goswami, Chapter 18, An alternative eco-friendly avenue for castor oil biodiesel:  
662 use of solid supported acidic salt catalyst, Chemical Science Block, CSIR- North-East  
663 Institute of Science & Technology, Assam, India, 380-396.
- 664 46. R. M. deAlmeida, L. K. Noda, N. S. Goncalves, S. M. P. Meneghetti, M. R.  
665 Meneghetti, Transesterification reaction of vegetable oils, using superacid sulfated  
666 TiO<sub>2</sub>-base catalysts, *Appl Catal A* 347 (2008), 100-105.
- 667 47. M. Rengasamy, K. Anbalagan, S. Kodhaiyolii and V. Pugalenthii, Castor leaf  
668 mediated synthesis of iron nanoparticles for evaluating catalytic effects in  
669 transesterification of castor oil, *RSC Adv* 6 (2016) 9261-9269.
- 670 48. H. Yuan, B. L. Yang, G. L. Zhu, Synthesis of biodiesel using microwave absorption  
671 catalysts, *Energy Fuels* 23 (2009) 548-552.
- 672 49. R. Liu, X. Wang, X. Zhao, P. Feng, Sulfonated ordered mesoporous carbon for  
673 catalytic preparation of biodiesel, *Carbon* 46 (2008) 1664-1669.
- 674 50. H.Y. Shrirame, N. L. Panwar, B.R. Bamniya, Biodiesel from castor oil- A Green Energy  
675 Option, *Low Carbon Economy* 2 (2011) 1-6.
- 676 51. M. L. Savaliya, B. Z. Dholakiya, A Simpler and highly efficient protocol for the  
677 preparation of biodiesel from soap stock oil using BBSA catalyst, *RSC Advances*, 5,  
678 (2015), 74416-74424.

**Declaration of interests**

- ✓  The authors declare that they have no known competing financial interests or personal relationships that could have appeared to influence the work reported in this paper.

The authors declare that they have no known competing financial interests or personal relationships that could have appeared to influence the work reported in this paper.

**Table 1. Physicochemical properties of castor oil [10-11]**

<b>Sr. No.</b>	<b>Properties</b>	<b>Value</b>
1.	FFA (%)	0.264
2.	Density (kg/m <sup>3</sup> )	962.8
3.	Fire point (°C)	335
4.	Flash point (°C)	298
5.	Cloud point (°C)	15.8
6.	Calorific value (kJ/kg)	35684.5
7.	Kinematic viscosity (mm <sup>2</sup> /s)	43.1
8.	Specific gravity	0.962
9.	Cetane number	40
10.	Iodine value (gI <sub>2</sub> /100g)	100

**Table 2. Results of castor biodiesel yield (%) with peculiar reaction parameters at 65 °C**

<b>Sr. No.</b>	<b>O:M molar ratio</b>	<b>Reaction time (h)</b>	<b>% (w/w) PTSA-Si</b>	<b>Biodiesel Yield* (%)</b>
1.	1:9	6	5 %	46.51 ± 0.93
2.	1:9	7	5%	59.36 ± 1.31
3.	1:9	8	5%	65.78 ± 0.70
4.	1:9	9	5%	72.32 ± 0.96
5.	1:9	10	5%	80.23 ± 0.91
6.	1:10	6	5%	58.98 ± 0.96
7.	1:10	7	5%	72.65 ± 0.89
8.	1:10	8	5%	79.25 ± 1.32
9.	1:10	9	5%	83.65 ± 0.78
10.	1:10	10	5%	88.12 ± 0.81
11.	1:11	6	5%	68.54 ± 0.91
12.	1:11	7	5%	80.29 ± 1.28
13.	1:11	8	5%	88.65 ± 1.21
14.	1:11	9	5%	91.32 ± 0.98
15.	1:11	10	5%	98.56 ± 0.99
16.	1:12	6	5%	66.32 ± 1.11
17.	1:12	7	5%	77.54 ± 0.78
18.	1:12	8	5%	86.32 ± 1.09
19.	1:12	9	5%	90.32 ± 1.16
20.	1:12	10	5%	94.23 ± 0.93
21.	1:11	10	1%	22.34 ± 1.31
22.	1:11	10	2%	38.35 ± 0.70
23.	1:11	10	3%	54.23 ± 1.11
24.	1:11	10	4%	82.56 ± 1.02
25.	1:11	10	6%	98.24 ± 0.98

\*(n=3) All experiments have been carried out in triplicates.

**Table 3. Results of specific surface area, pore volume and pore size of PTSA-Si**

<b>Sr. No.</b>	<b>Catalyst</b>	<b>Specific surface area (m<sup>2</sup>/g)</b>	<b>Pore volume (P/Po) (cm<sup>3</sup>/g)</b>	<b>Pore size (nm)</b>
1.	PTSA-Si	9.61	0.99	2.50

**Table 4. Physico-chemical properties of PTSA-Si**

<b>Sr. No.</b>	<b>Catalyst</b>	<b>Temperature at maximum (°C)</b>	<b>Acidity) (mmol/g)</b>	<b>Volume (mL/g STP)</b>
1.	PTSA-Si	194.8	1.49	6.94



**Table 5. Comparison of catalytic activity of PTSA-Si with reported results (Feedstock: Castor oil)**

Sr. No	Catalyst	Reaction Conditions				Biodiesel yield (%)	Ref.
		Reaction Temp. (°C)	Catalyst % (w/w)	O:M molar ratio	Reaction time (h)		
1.	PTSA-Si	65	5.0	1:11	10	98.56	Present study
2.	Iron (II) doped zinc oxide nanocatalyst	55	14	1:12	50 min.	91.0	[40]
3.	Sulphonated phenyl silane montmorillonite	60	5.0	1:12	300 min.	89.8	[41]
4.	Super acidic sulfonated modified mica catalyst	60	6.0	1:12	300 min.	90.0	[42]
5.	Supported polyaniline-sulfate	55	4.3	1:29	10	78.0	[43]
6.	Tin (IV) complexes	150	1.0	1:4	4.0	61.0	[44]
7.	Solid supported acidic salt catalyst	70	5.0	1:40	5.0	95.0	[45]
8.	sulfated titania	120	1.0	1:6	1.0	25.0	[46]
9.	Iron nanocatalyst	65	1.0	1:9	150 min.	85.0	[47]
10.	Sulfonated activated-carbons	65	5.0	1:12	60 min	94.0	[48]

**Table 6. Fuel properties of castor biodiesel in contrast to ASTM standards**

<b>Entry No.</b>	<b>Properties</b>	<b>Biodiesel</b>	<b>ASTM Limits</b>	<b>Standard method</b>
1.	Density (40 °C) kg/m <sup>3</sup>	872	860-900	EN14214-2008
2.	Flash point (°C)	168	>130	ASTM D92
3.	Kinematic viscosity at 40°C (mm <sup>2</sup> /s)	6.12	1.9-6.0	ASTM D 6751-12
4.	Cetane index	49.85	52.0	ASTM D 976
5.	Cloud point (°C)	-3.4	-15 to 5	ASTM D 2500
6.	Net calorific value (MJ/kg)	40.20	-	IS 1448 P 33 1991
7.	Fire point (°C)	175	>140	ASTM D94
8.	Specific gravity	0.87	0.860–0.900	ASTM D 4052
9.	Acid value (mgKOH/g)	0.64	0.8	ASTM D 6751-09
10	Iodine value (g I <sub>2</sub> /100 g oil)	83.24	120	EN14214-2008
11.	Pour point (°C)	-19	-15	ASTM D97
12.	Refractive index	1.45	-	ASTM D 960-79

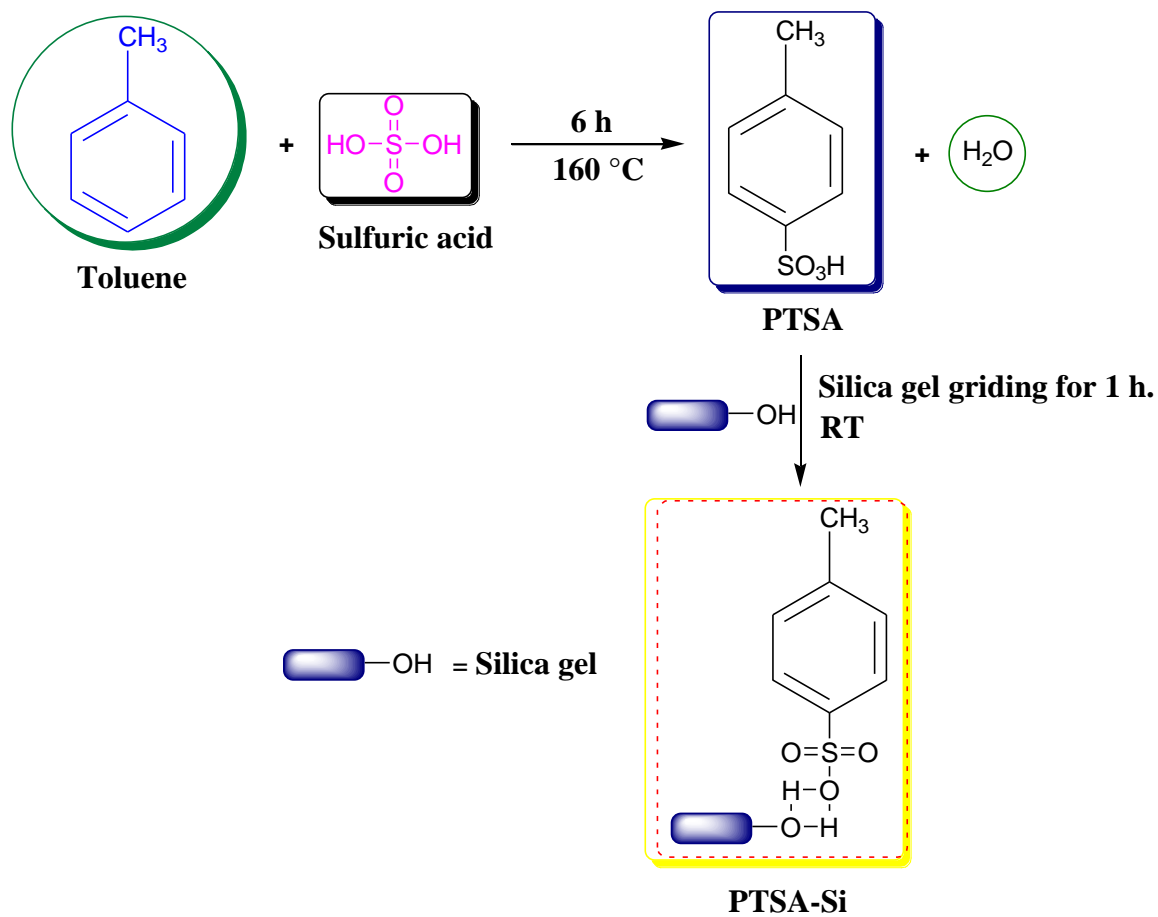
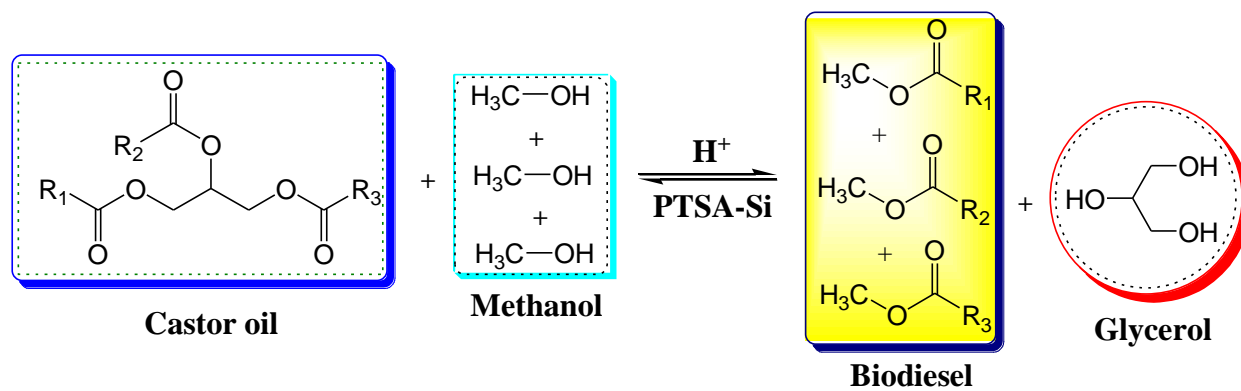
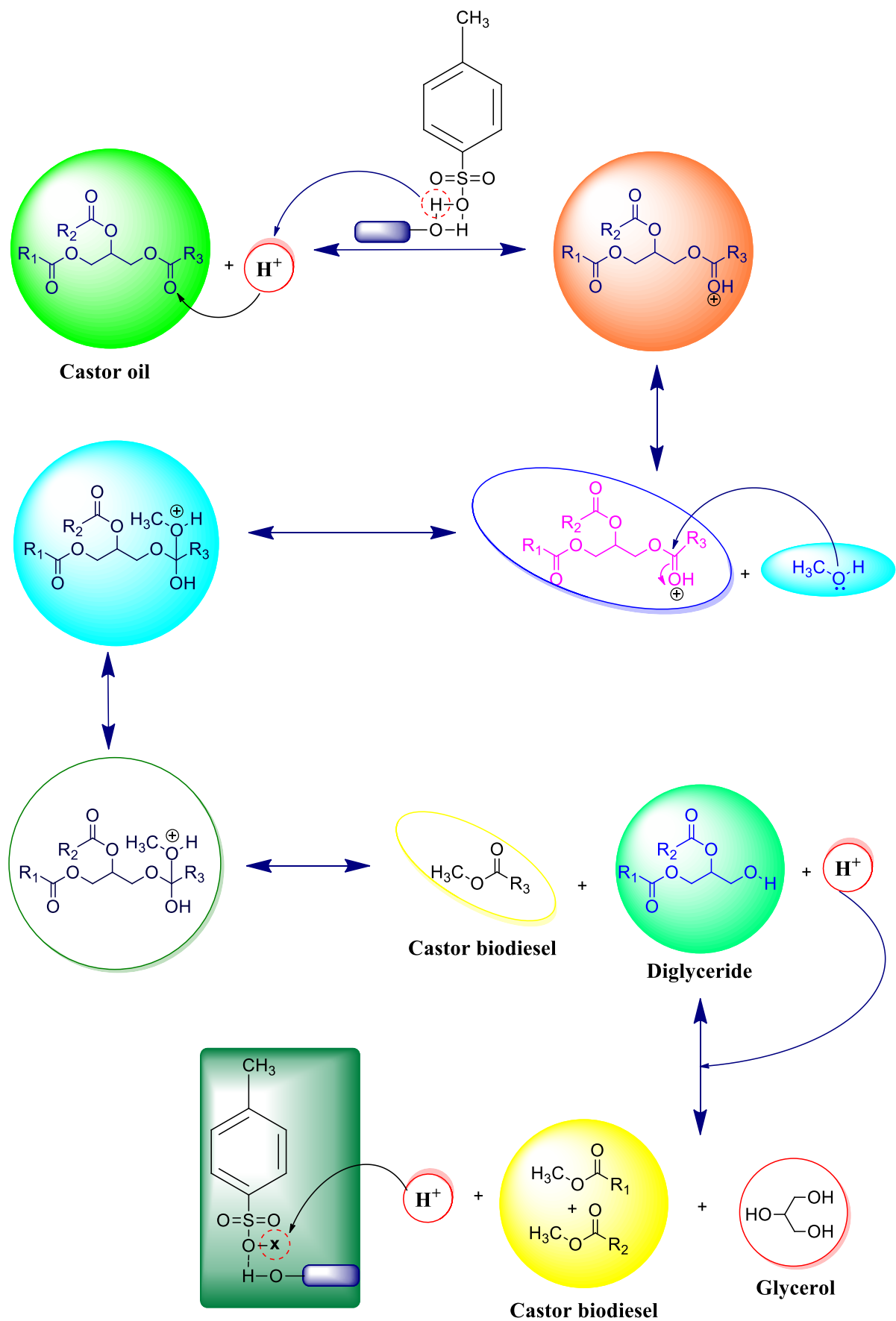


Fig. 1. Reaction scheme for the preparation of PTSA-Si catalyst



**Fig. 2.** Reaction scheme for the transesterification of castor oil to biodiesel



**Fig. 3. Proposed reaction mechanism for the transesterification of castor oil to biodiesel**

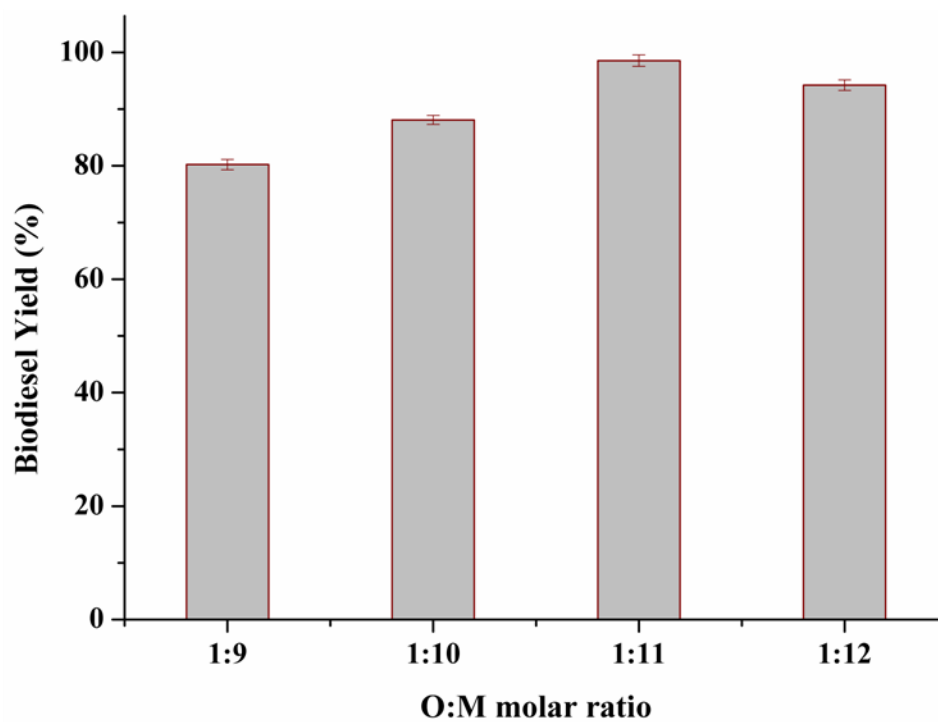


**Fig. 4.** Impact of oil to methanol molar ratio on the (%) yield of biodiesel (Reaction time: 10 h and PTSA-Si: 5 % (*w/w*))

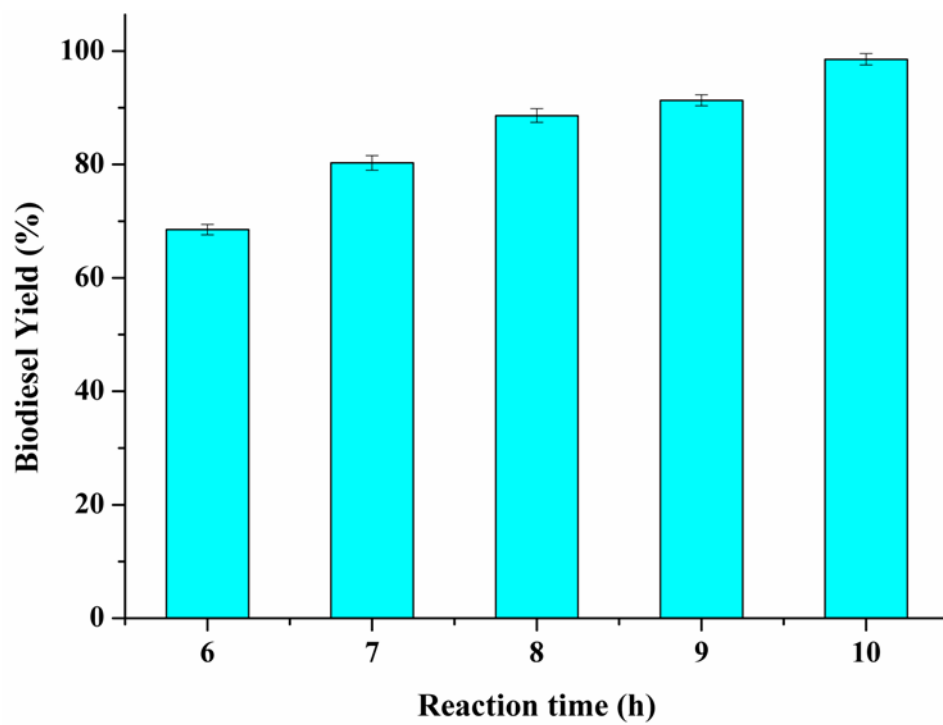


**Fig. 5. Impact of reaction time (h) on the (%) yield of biodiesel (O:M molar ratio: 1:12 and PTSA-Si: 5 % (w/w))**

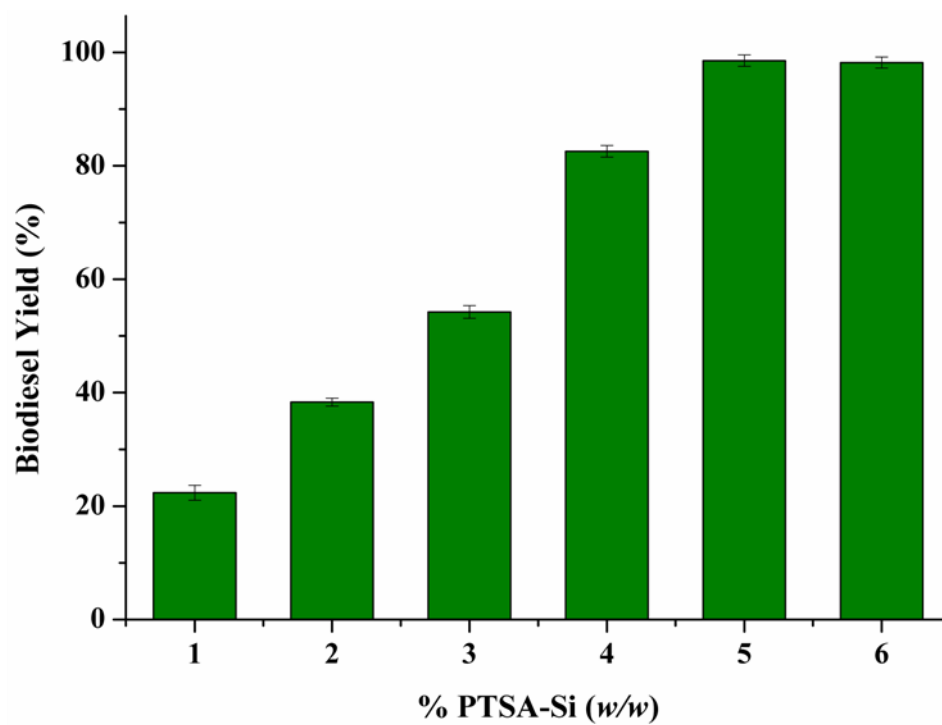


**Fig. 6. Impact of % PTSA-Si (*w/w*) on the (%) yield of biodiesel (O:M molar ratio: 1:11 and Reaction time: 10 h)**



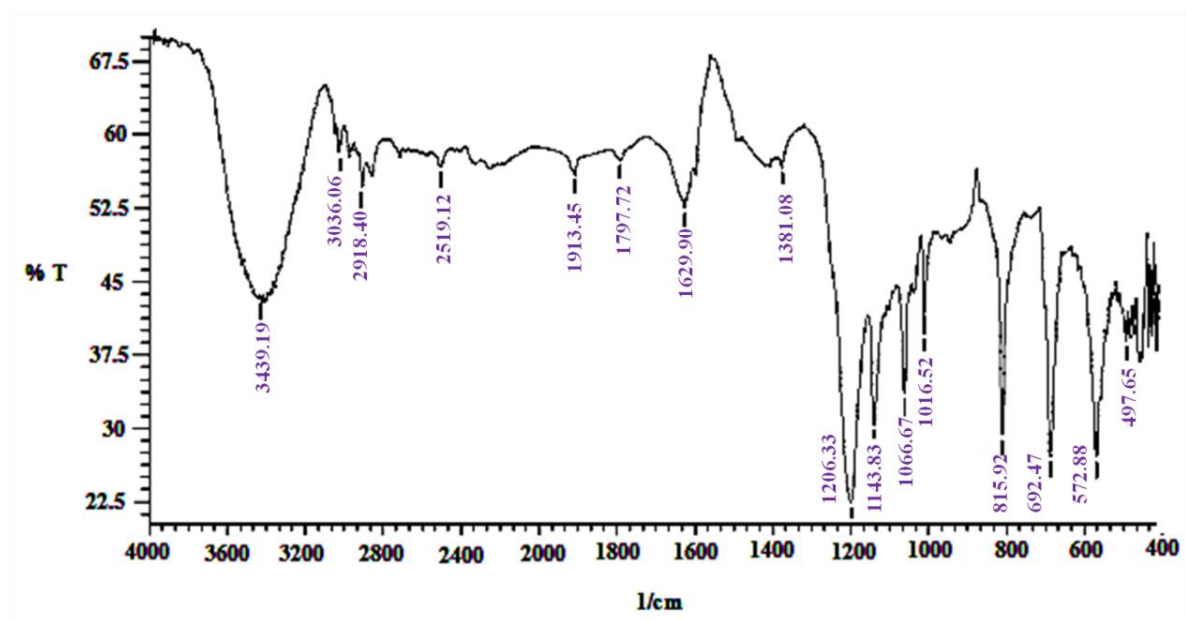
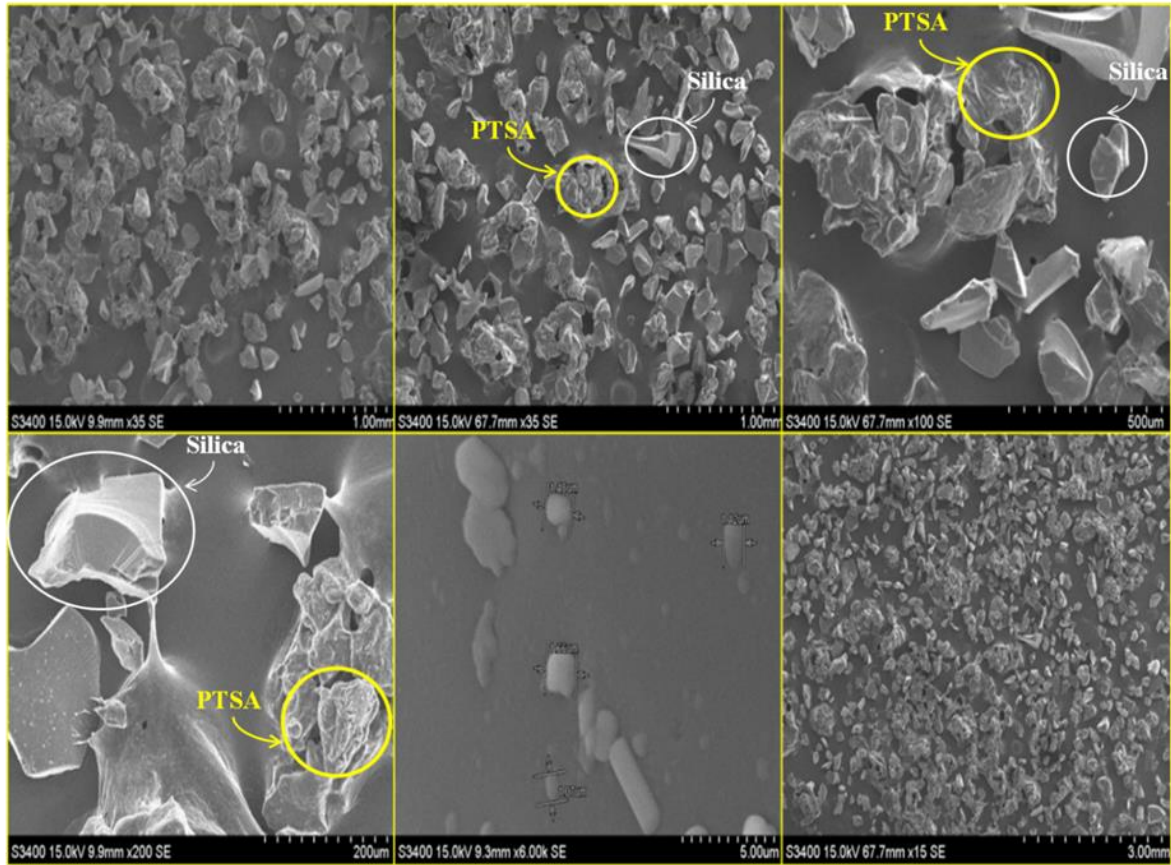
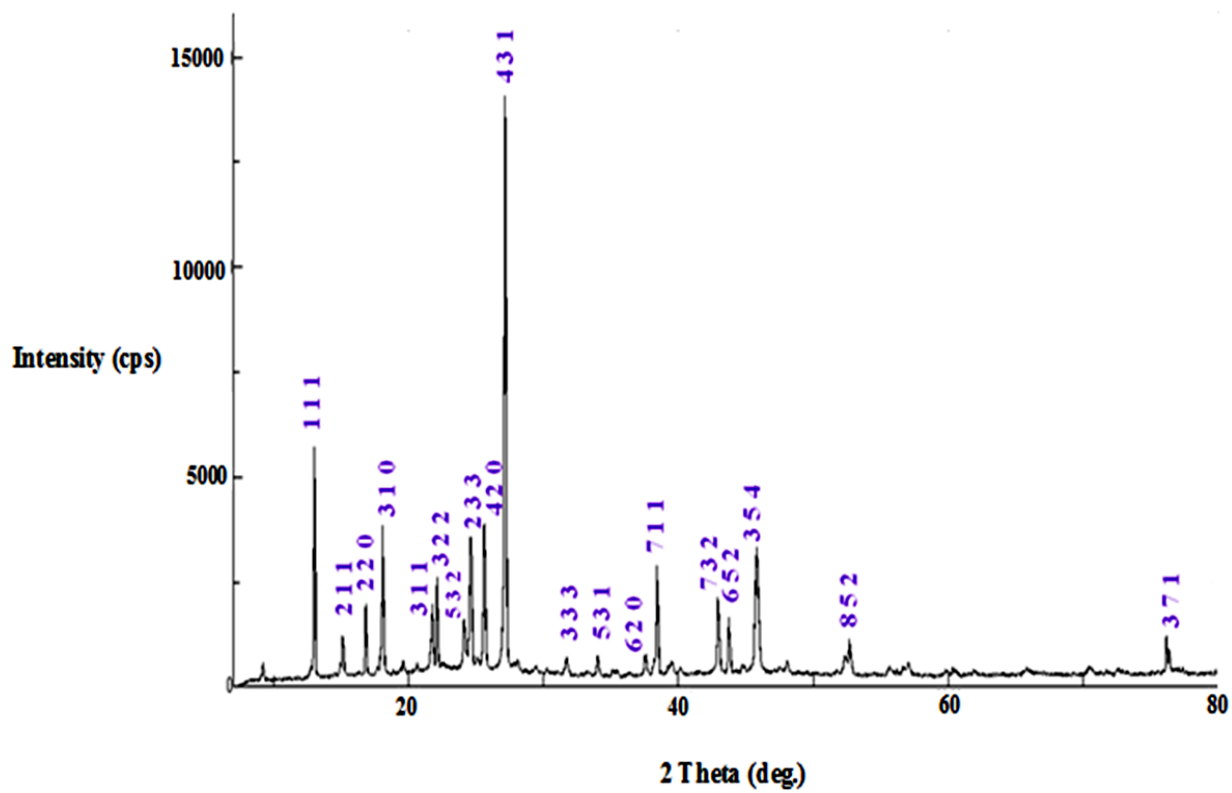


Fig. 7. FT-IR spectrum of PTSA-Si



**Fig. 8. SEM micrographs of PTSA-Si**



**Fig. 9.** The wide angle X-Ray diffractogram of PTSA-Si

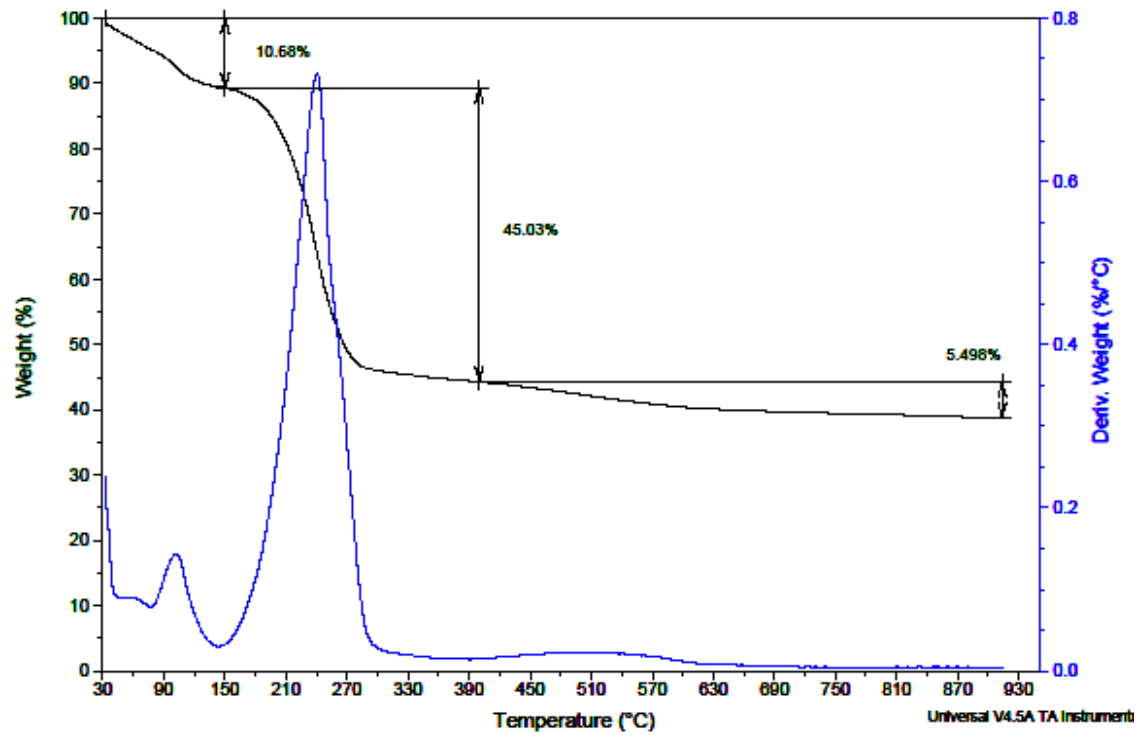


Fig. 10. TGA-DTA profile of PTSA-Si

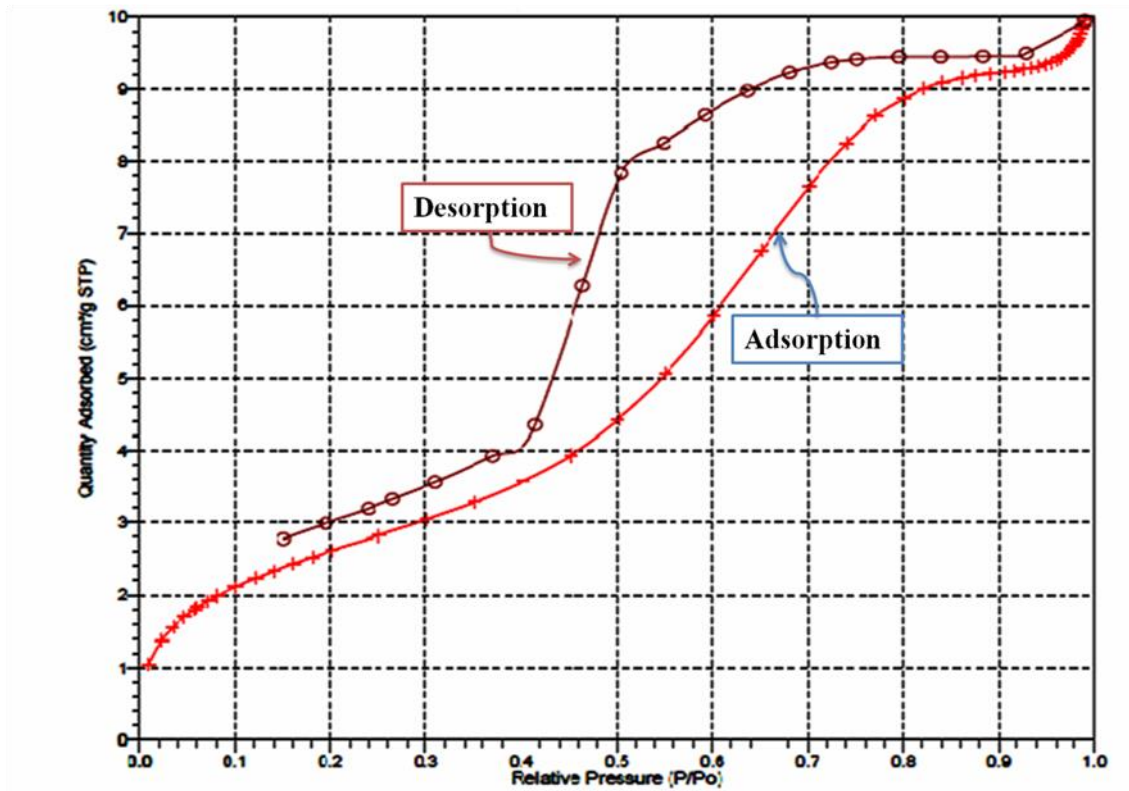
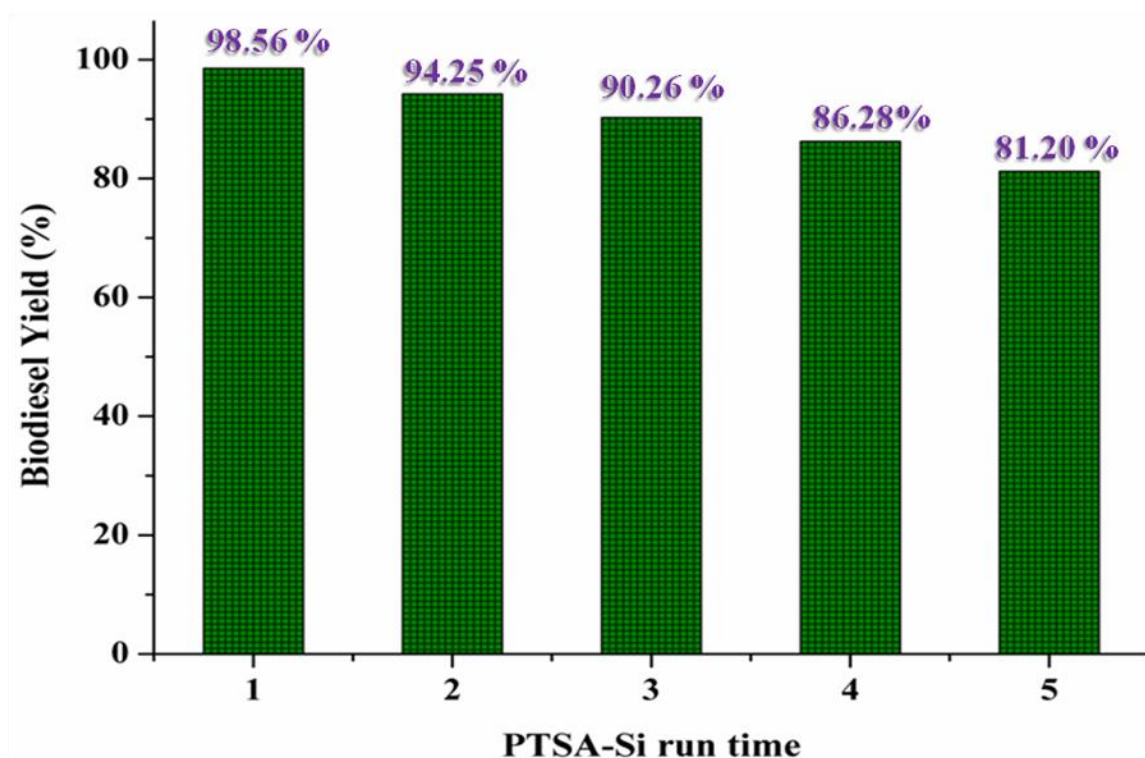


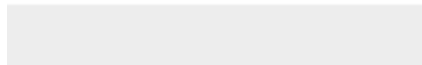
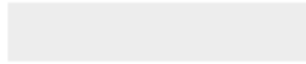
Fig. 11. BET profile of PTSA-Si



**Fig. 12.** Impact of PTSA-Si runs time on the (%) yield of biodiesel ((i) 1:11 oil to methanol molar ratio, (ii) 5 % PTSA-Si catalyst (*w/w*), (iii) 65 °C reaction temperature and (iv) 10 h reaction time)



Click here to access/download  
**Supplementary Material**  
Supporting information file.docx





[Click here to access/download](#)

**Data in Brief**  
Nomenclature.docx

